Solution-based intramolecular singlet fission in cross-conjugated pentacene dimers

Johannes Zirzlmeier,[a] Rubén Casillas,[a] S. Rajagopala Reddy,[b] Pedro B. Coto,[b] Dan Lehnherr,[c] Erin T. Chernick,[d] Ilias Papadopoulos,[a] Michael Thoss,[b] Rik R. Tykwinski*[d] and Dirk M. Guldi*[a]

[a]Department of Chemistry and Pharmacy & Interdisciplinary Center for Molecular Materials (ICMM), Engineering of Advanced Materials (EAM), Friedrich-Alexander-Universität Erlangen-Nürnberg (FAU), Egerlandstrasse 3, 91058 Erlangen, Germany
[b]Institute for Theoretical Physics & Interdisciplinary Center for Molecular Materials, Friedrich-Alexander-Universität Erlangen-Nürnberg (FAU), Staudtstrasse 7/B2, 91058 Erlangen, Germany
[c]Department of Chemistry, University of Alberta, Edmonton, Alberta, T6G 2G2, Canada
[d]Department of Chemistry and Pharmacy & Interdisciplinary Center for Molecular Materials (ICMM), Friedrich-Alexander-Universität Erlangen-Nürnberg (FAU), Henkestrasse 42, 91054 Erlangen, Germany

Table of Contents

General procedures and methods

Reagents were purchased in reagent grade from commercial suppliers and used without further purification. The synthesis of **1**,[1] **2**,[2] **3**,[3] **6**,[4] and **7**[5] has been previously reported. THF was distilled from sodium/benzophenone ketyl. Anhydrous $MgSO_4$ was used as the drying agent after aqueous work-up. Evaporation and concentration *in vacuo* was done at water-aspirator pressure. All reactions were performed in standard, dry glassware under an inert atmosphere of nitrogen or argon. Column chromatography: silica gel-60 (230–400 mesh). Thin Layer Chromatography (TLC): pre-coated plastic sheets covered with 0.20 mm silica gel with fluorescent indicator UV 254 nm; visualization by UV light or $KMnO_4$ stain. Melting points are uncorrected.

Proton nuclear magnetic resonance (^{1}H NMR) spectra and carbon nuclear magnetic resonance (^{13}C NMR) spectra were recorded at 27 °C in $CDCl_3$; solvent peaks (7.24 for ^{1}H and 77.0 for ^{13}C) as reference (unless stated otherwise) on Varian-Mercury-400 (400 MHz), Bruker Advance (400 MHz), or Varian Unity/Inova 500 (500 MHz) spectrometer. Coupling constants are reported as observed (±0.5 Hz).

All electrochemical measurements were performed with a Metrohm FRA 2 μAutolab Type III potentiostat. A single-compartment, three electrode cell configuration was used for the square wave voltammetry measurements, using a glassy carbon electrode (3 mm diameter) as a working electrode, a platinum wire as a counter and a silver wire as a reference electrode. Steady state UV-vis absorption spectra were acquired at rt using a Perkin Elmer Lambda 2 spectrometer and a Varian Cary 400 spectrometer. Steady state fluorescence spectra were carried out at a FluoroMax3 spectrometer from Horiba in the visible detection range (rt) and at a FluoroLog3 spectrometer from Horiba with a IGA Symphony detector in the NIR (77K). Femtosecond transient absorption (TA) experiments were carried out with an amplified Ti:Sapphire CPA-2110 fs laser system (Clark MXR: output 775 nm, 1 kHz, 150 fs pulse width) using transient absorption pump/probe detection systems (Helios and Eos, Ultrafast Systems) with argon-purged solutions. The 480 and 656 nm excitation wavelengths were generated with a noncolinear optical parametric amplifier (NOPA, Clark MXR). The 387 nm excitation wavelength was generated via SHG of the 775 nm laser output.

Femtosecond transient absorption data were fitted using multiwavelength analysis with Origin (OriginLab, Northampton, MA) or global analysis. The global fitting was performed with the

open-source software package Glotaran.[6] The latter is a free, Java-based graphical user interface to the R package TIMP, developed for global and target analysis of time-resolved spectroscopy. The wavelength dependent character (dispersion) of the instrument response function (IRF) was modeled and taken into account.

For mass spectral analyses, low-resolution data are provided in cases when M^+ is not the base peak; otherwise, only high-resolution data are provided. MALDI mass spectrometry used the matrix *trans*-2-[3-(4-*tert*-butylphenyl)-2-methyl-2-propenylidene]malononitrile (DCTB).

Differential scanning calorimetry (DSC) measurements were measured on a Perkin Elmer Pyris 1 DSC instrument. Thermogravometric analyses (TGA) were carried out on a Perkin Elmer Pyris 1 TGA instrument. All thermal analyses were carried out under a flow of nitrogen with a heating rate of 10 °C/min. Thermal decomposition temperature as measured by TGA (as sample weight loss) are reported as T_d in which the temperature listed corresponds to the intersection of the tangent lines of the baseline and the edge of the peak corresponding to the first significant weight loss, typically >5%. Melting points from DSC analysis are reported as the peak maxima, except in cases when the sample decomposed, in which case the onset temperature of the decomposition exothermic peak is reported, as well as the exothermic maxima corresponding to the decomposition.

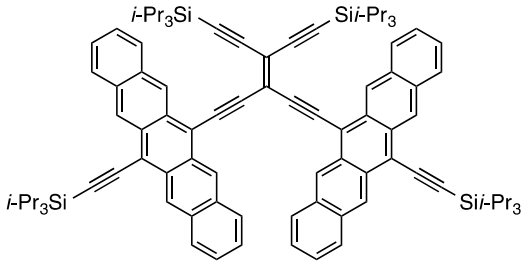

XC1: To a solution of **4** (0.265 g, 0.178 mmol) in dry THF (12 mL) that had been deoxygenated by bubbling argon for 2 min was added $SnCl_2 \cdot 2H_2O$ (0.112 g, 0.496 mmol) followed by 10% aq. H_2SO_4 (0.10 mL; prepared by adding 10 mL of conc. H_2SO_4 in 90 mL H_2O). The reaction flask was wrapped in aluminum foil to limit light exposure. This mixture was further deoxygenated for ca. 2 min. The solution was stirred at rt for a 5.5 h, poured onto a pad of silica gel (8 cm diameter × 4 cm thick), eluted with 2:1 hexanes/CH_2Cl_2, and the solvent was removed *in vacuo*. Column chromatography (silica gel, 4:1 hexanes/CH_2Cl_2) afforded **XC1** (0.198 g, 82%) as a blue solid. R_f = 0.74 (4:1 hexanes/CH_2Cl_2). UV-vis (CH_2Cl_2) λ_{max} (ε): 271 (58 800), 310 (332 000), 437 (24 900), 569 (sh, 9 370), 626 (sh, 24 300), 673 (36 100) nm. IR (CH_2Cl_2 cast film): 3049 (w), 2942 (w), 2890 (m), 2864 (m), 2129 (m) cm^{-1}. ^1H NMR (500 MHz, $CDCl_3$): δ 9.39 (s, 4H), 9.31 (s, 4H), 7.94 (d, *J* = 8.4 Hz, 4H), 7.84 (d, *J* = 8.4 Hz, 4H), 7.35 (t, *J* = 7.4 Hz, 4H), 7.21 (t, *J* = 7.3 Hz, 4H), 1.48–1.34 (m, 42H), 1.10–0.94 (m, 42H). ^{13}C NMR (125 MHz, $CDCl_3$): δ 132.4, 132.3, 130.6, 130.5, 128.8, 128.5, 126.4, 126.2, 126.0, 125.9, 119.6, 117.7, 117.2, 116.7, 107.9, 104.73, 104.71, 104.1, 102.0, 97.8, 19.0, 18.5, 11.7, 11.3. MALDI HRMS *m/z* calcd. for $C_{94}H_{108}Si_4$ (M^+) 1348.7523, found 1348.7514. TGA: $T_d \approx 365$ °C. DSC: decomposition, 269 °C (onset), 277 °C (peak).

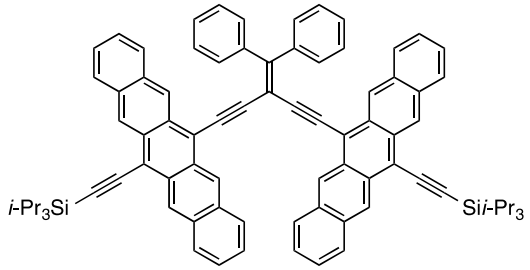

XC2: To a solution of **5** (0.240 g, 0.190 mmol) in dry THF (10 mL) that had been deoxygenated by bubbling argon for 2 min was added $SnCl_2 \cdot 2H_2O$ (0.231 g, 1.02 mmol) followed by 10% aq. H_2SO_4 (0.10 mL; prepared by adding 10 mL of conc. H_2SO_4 in 90 mL H_2O). The reaction flask was wrapped in aluminum foil to limit light exposure. This mixture was further deoxygenated for ca. 2 min. The solution was stirred at rt for a 5.5 h, poured onto a pad of silica gel (8 cm diameter × 4 cm thick), eluted with 3:1 hexanes/CH_2Cl_2, and the solvent was removed *in vacuo*. Column chromatography (silica gel, 3:1 hexanes/CH_2Cl_2) afforded **XC2** (0.205 g, 95%) as a blue solid. R_f = 0.59 (3:1 hexanes/CH_2Cl_2). UV-vis (CH_2Cl_2) λ_{max} (ε): 249 (49 400), 273 (53 800), 315 (268 000), 349 (sh, 18 100), 415 (23 400), 440 (sh, 10 500), 575 (9 920), 620 (27 000), 677 (48 400) nm. IR (microscope): 3050 (s), 2941 (s), 2889 (s), 2864 (s), 2126 (s) cm^{-1}. ^1H NMR (500 MHz, $CDCl_3$): δ 9.31 (s, 4H), 9.10 (s, 4H), 8.00–7.95 (m, 4H), 7.92 (d, J = 8.6 Hz, 4H), 7.60–7.54 (m, 6H), 7.34 (d, J = 8.6 Hz, 4H), 7.27 (t, J = 7.5 Hz, 4H), 6.96 (t, J = 7.5 Hz, 4H), 1.48–1.38 (m, 42H). ^{13}C NMR (125 MHz, $CDCl_3$): δ 155.4, 141.1, 132.33, 132.28, 131.1, 130.6, 130.5, 129.6, 128.8, 128.4, 128.3, 126.3, 125.92, 125.90, 125.5, 118.5, 118.0, 107.4, 104.9, 104.8, 103.7, 91.7, 19.0, 11.7. ^{13}C NMR (APT, 125 MHz, $CDCl_3$): δ 155.4 (C), 141.1 (C), 132.33 (C), 132.28 (C), 131.1 (CH), 130.6 (C), 130.5 (C), 129.6 (CH), 128.8 (CH), 128.4 (CH), 128.3 (CH), 126.3 (CH), 125.92 (CH), 125.90 (CH), 125.5 (CH), 118.5 (C), 118.0 (C), 107.4 (C), 104.9 (C), 104.8 (C), 103.7 (C), 91.7 (C), 19.0 (CH_3), 11.7 (CH). MALDI HRMS m/z calcd. for $C_{84}H_{76}Si_2$ (M^+) 1140.5480, found 1140.5465. TGA: $T_d \approx$ 405 °C. DSC: decomposition, 154 °C (onset), 187 °C (peak).

X-ray data for **XC2** (CCDC 1417348): $C_{84}H_{76}Si_2 \bullet 1.5C_4H_8O$, M_r = 1249.78 g mol^{-1}; crystal dimensions (mm) 0.85 × 0.61 × 0.21; monoclinic space group $I2/a$ (an alternate setting of $C2/c$ [No. 15]); a = 30.224 (5) Å, b = 15.151 (2) Å, c = 31.687 (5) Å; β = 96.672 (2)°; V = 14412 (4) $Å^3$; Z = 8; ρ_{calcd} = 1.152 g cm^{-3}; μ = 0.098 mm^{-1}; λ = 0.71073 Å; T = –100 °C; $2\theta_{max}$ = 51.90°; total data collected = 52527; R_1 = 0.0701 [7295 observed reflections with $F_o^2 \geq 2\sigma(F_o^2)$]; wR_2 = 0.0.2338 for

831variables, 13814 unique reflections, and 12 variables; residual electron density = 0.438 and –0.326 e $Å^{-3}$.

Two different sets of constraints were applied to bond distances involving the disordered silyl-isopropyl groups: (a) the Si–C distances (d(Si1–C31A), d(Si1–C31B), d(Si2–C82A), d(Si2–C82A)) were constrained to be equal (within 0.03 Å) to a common refined value during refinement; (b) the C–C distances (d(C31A–C32A), d(C31A–C33A), d(C31B–C32B), d(C31B–C33B), d(C82A–C83A), d(C82A–C84A), d(C82B–C83B), d(C82B–C84B)) were constrained to be equal (within 0.03 Å) to a common refined value during refinement.

Attempts to refine peaks of residual electron density as disordered or partial-occupancy solvent tetrahydrofuran oxygen or carbon atoms were unsuccessful. The data were corrected for disordered electron density through use of the SQUEEZE procedure as implemented in *PLATON* (Spek, A. L. *Acta Crystallogr.* **2015**, *C71*, 9–18. *PLATON* - a multipurpose crystallographic tool. Utrecht University, Utrecht, The Netherlands). A total solvent-accessible void volume of 2361.8 $Å^3$ with a total electron count of 483 (consistent with 12 molecules of solvent tetrahydrofuran, or 1.5 molecules of THF per formula unit of the molecule of interest) was found in the unit cell.

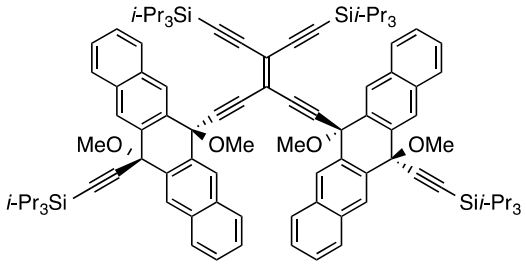

4: To a solution of **1** (0.414 g, 0.760 mmol) and 1,1-dibromo-2,2-bis(triisopropylsilylethynyl)ethene (**2**, 0.174 g, 0.318 mmol) in dry THF (6 mL) and diisopropylamine (8.0 mL, 4.3 g, 42 mmol) which had been deoxygenated for 10 min with argon was added $Pd(PPh_3)_4$ (0.034 g, 0.029 mmol) and CuCl (0.06 g, 0.06 mmol). The reaction mixture was further deoxygenated with argon for an additional 2 min. The reaction mixture was stirred for 16 h at 50–60 °C, cooled to rt, and poured into satd. aq. NH_4Cl (150 mL). H_2O (50 mL) was added and the mixture was extracted with CH_2Cl_2 (80 mL, 50 mL). The organic phase was washed with 5% NH_4Cl (200 mL), satd. aq. NaCl (150 mL), dried ($MgSO_4$), filtered, and the solvent removed *in vacuo*. Column chromatography (silica gel, 9:1 hexanes/EtOAc) afforded **4** (0.299 g, 63%) as an off white foamy solid. R_f = 0.43 (9:1 hexanes/EtOAc). IR (microscope): 3056 (w), 2943 (s), 2891 (m), 2865 (s), 2166 (vw), 2144 (vw), 1463 (m) cm^{-1}. ^1H NMR (500 MHz, $CDCl_3$): δ 8.49 (s, 4H), 8.31 (s, 4H), 7.86 (d, *J* = 7.9 Hz, 4H), 7.80 (d, *J* = 8.0 Hz, 4H), 7.55–7.49 (m, 4H), 7.49–7.44 (m, 4H), 3.03 (s, 6H), 2.65 (s, 6H), 1.19–1.12 (m, 42H), 1.00–0.92 (m, 42H). ^{13}C NMR (125 MHz, $CDCl_3$): δ 133.8, 133.5, 133.1, 132.9, 128.2, 128.0, 127.7, 127.0, 126.5, 117.6, 116.1, 106.5, 103.6, 102.0, 99.1, 90.1, 84.4, 75.2, 74.4, 52.4, 51.6, 18.7, 18.5, 11.3, 11.1 (one signal coincident or not observed). ^{13}C NMR (APT, 125 MHz, $CDCl_3$): δ 133.8 (C), 133.5 (C), 133.1 (C), 132.8 (C), 128.2 (CH), 128.0 (CH), 127.7 (CH), 127.0 (CH), 126.5 (CH), 117.6 (C), 116.1 (C), 106.5 (C), 103.6 (C), 102.0 (C), 99.1 (C), 90.1 (C), 84.4 (C), 75.2 (C), 74.4 (C), 52.4 (CH_3), 51.6 (CH_3), 18.7 (CH), 18.5 (CH), 11.3 (CH), 11.1 (CH) (one signal coincident or not observed). MALDI MS *m/z* 1472.8 (M^+, 83), 1441.8 ([M – OCH_3]$^+$, 100). MALDI HRMS *m/z* calcd. for $C_{98}H_{120}O_4Si_4$ (M^+) 1472.8258, found 1472.8253.

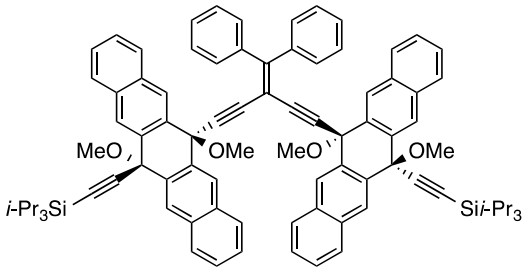

5: To a solution of **1** (0.419 g, 0.769 mmol) and 1,1-dibromo-2,2-diphenylethene (**3**, 0.111 g, 0.328 mmol) in dry THF (6 mL) and diisopropylamine (8.0 mL, 4.3 g, 42 mmol) which had been deoxygenated for 10 min with argon was added $Pd(PPh_3)_4$ (0.030 g, 0.026 mmol) and CuCl (0.05 g, 0.05 mmol). The reaction mixture was further deoxygenated with argon for an additional 2 min. The reaction mixture was stirred for 16 h at 50–60 °C, cooled to rt, and poured into satd. aq. NH_4Cl (150 mL). H_2O (50 mL) was added and the mixture was extracted with CH_2Cl_2 (80 mL, 50 mL). The organic phase was washed with 5% NH_4Cl (200 mL), satd. aq. NaCl (150 mL), dried ($MgSO_4$), filtered, and the solvent removed *in vacuo*. Column chromatography (silica gel, 9:1 hexanes/EtOAc) afforded **5** (0.248 g, 60%) as an off white foamy solid. R_f = 0.22 (9:1 hexanes/EtOAc), 0.39 (2:1 CH_2Cl_2/hexanes). IR ($CDCl_3$ cast film): 3056 (m), 2943 (s), 2891 (m), 2865 (s), 2247 (w), 2167 (w) cm^{-1}. ^1H NMR (500 MHz, $CDCl_3$): δ 8.53 (s, 4H), 8.18 (s, 4H), 7.89 (d, *J* = 8.2 Hz, 4H), 7.71 (d, *J* = 8.2 Hz, 4H), 7.53 (dt, *J* = 1.1 Hz, 7.4 Hz, 4H), 7.36 (dt, *J* = 1.1 Hz, 7.5 Hz, 4H), 7.19 (d, *J* = 7.2 Hz, 4H), 6.97 (tt, *J* = 1.2 Hz, 7.4 Hz, 2H), 6.86 (t, *J* = 7.7 Hz, 4H), 2.88 (s, 6H), 2.66 (s, 6H), 1.20–1.10 (m, 42H). ^{13}C NMR (125 MHz, $CDCl_3$): δ 133.5, 133.4, 133.2, 132.9, 130.2, 128.2, 128.1, 127.9, 127.4, 127.2, 126.51, 126.46, 106.8, 101.09, 92.1, 90.1, 85.9, 75.0, 73.9, 51.9, 51.5, 18.7, 11.3 (three signals coincident or not observed). MALDI HRMS *m/z* calcd. for $C_{88}H_{88}O_4Si_2$ (M^+) 1264.6216, found 1264.62.

Experimental data and compound characterization

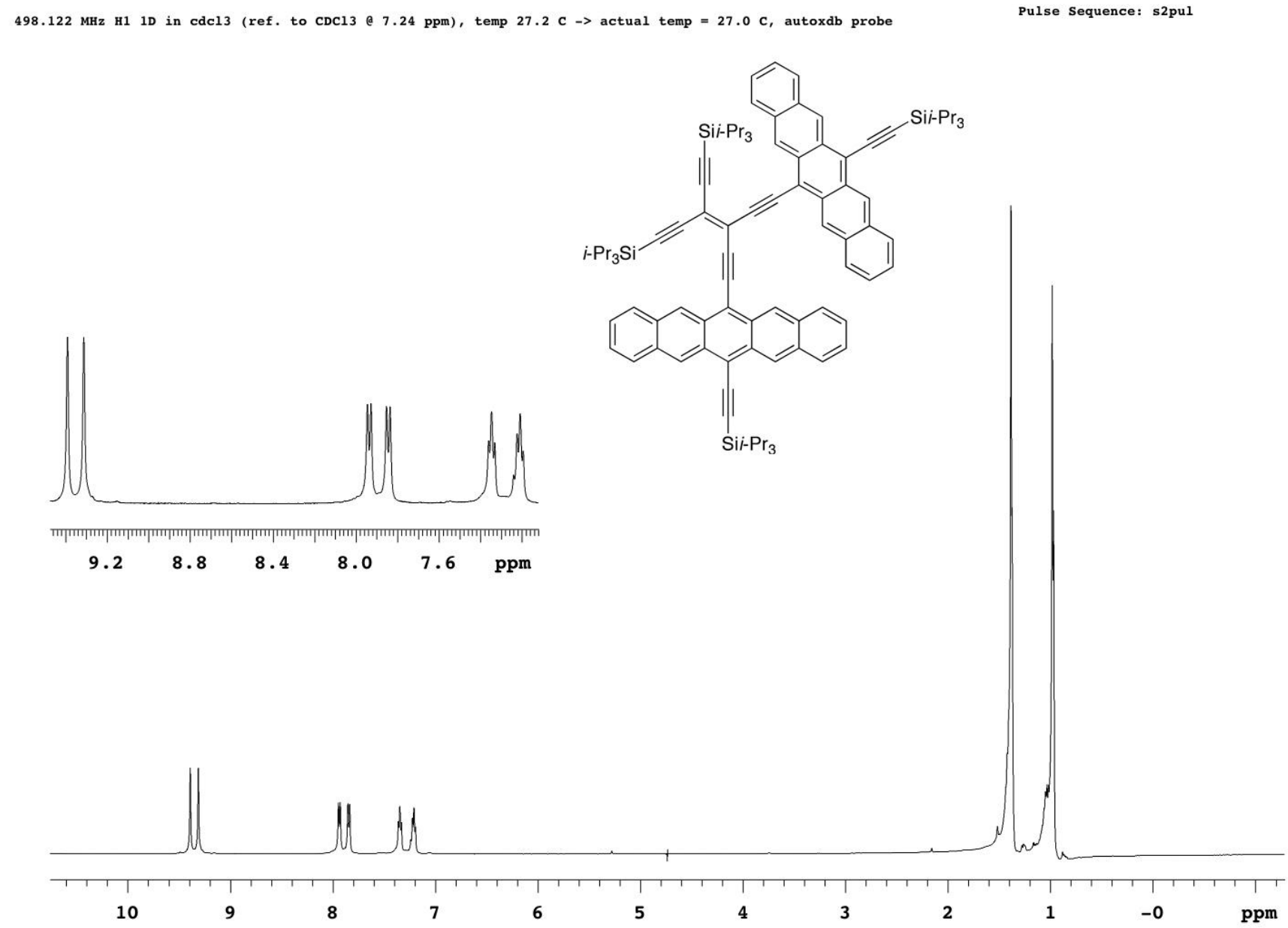

Figure S1: ^{1}H NMR (500 MHz) spectrum of **XC1** in $CDCl_3$.

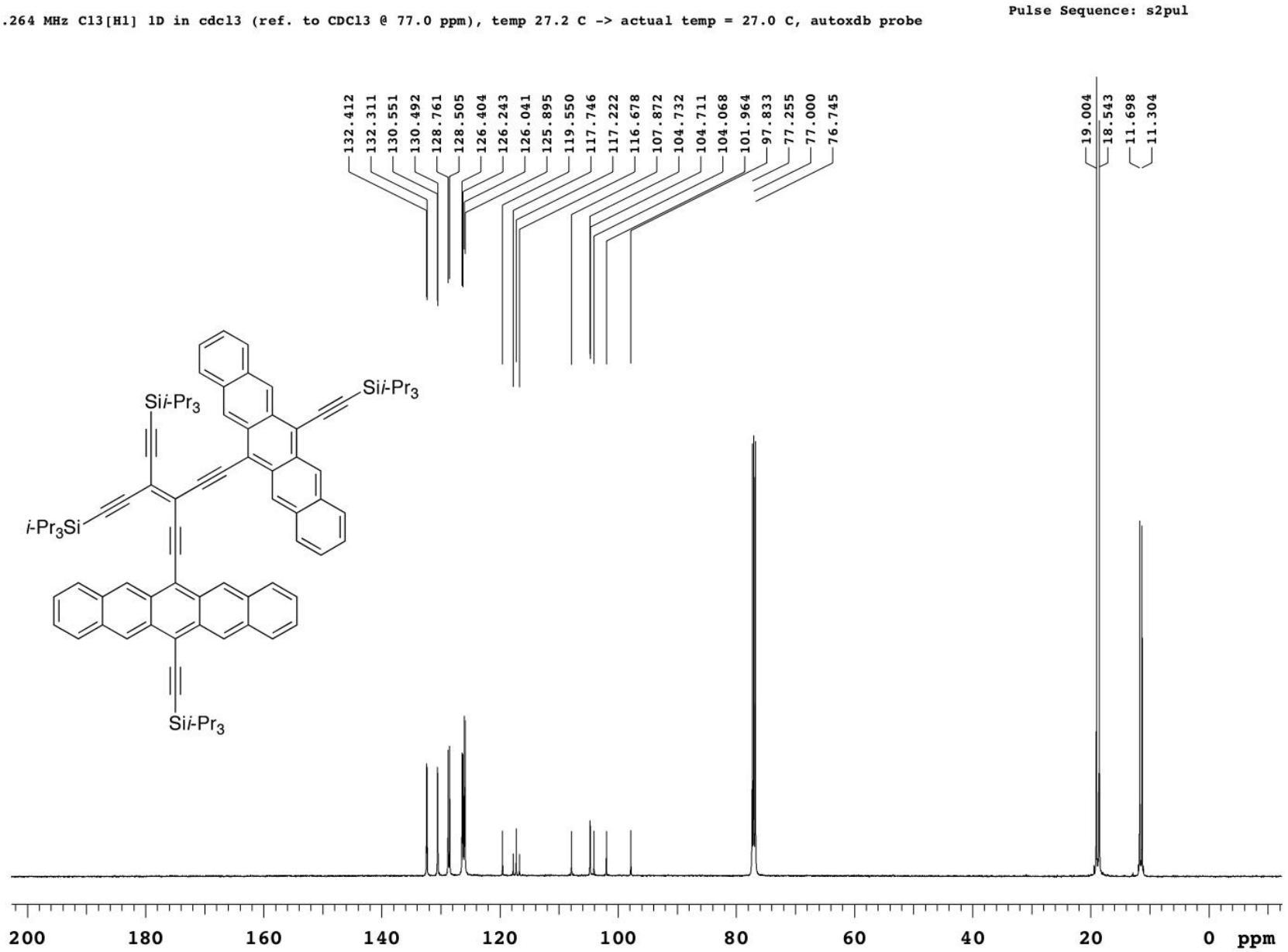

Figure S2: ^{13}C NMR (500 MHz) spectrum of **XC1** in $CDCl_3$.

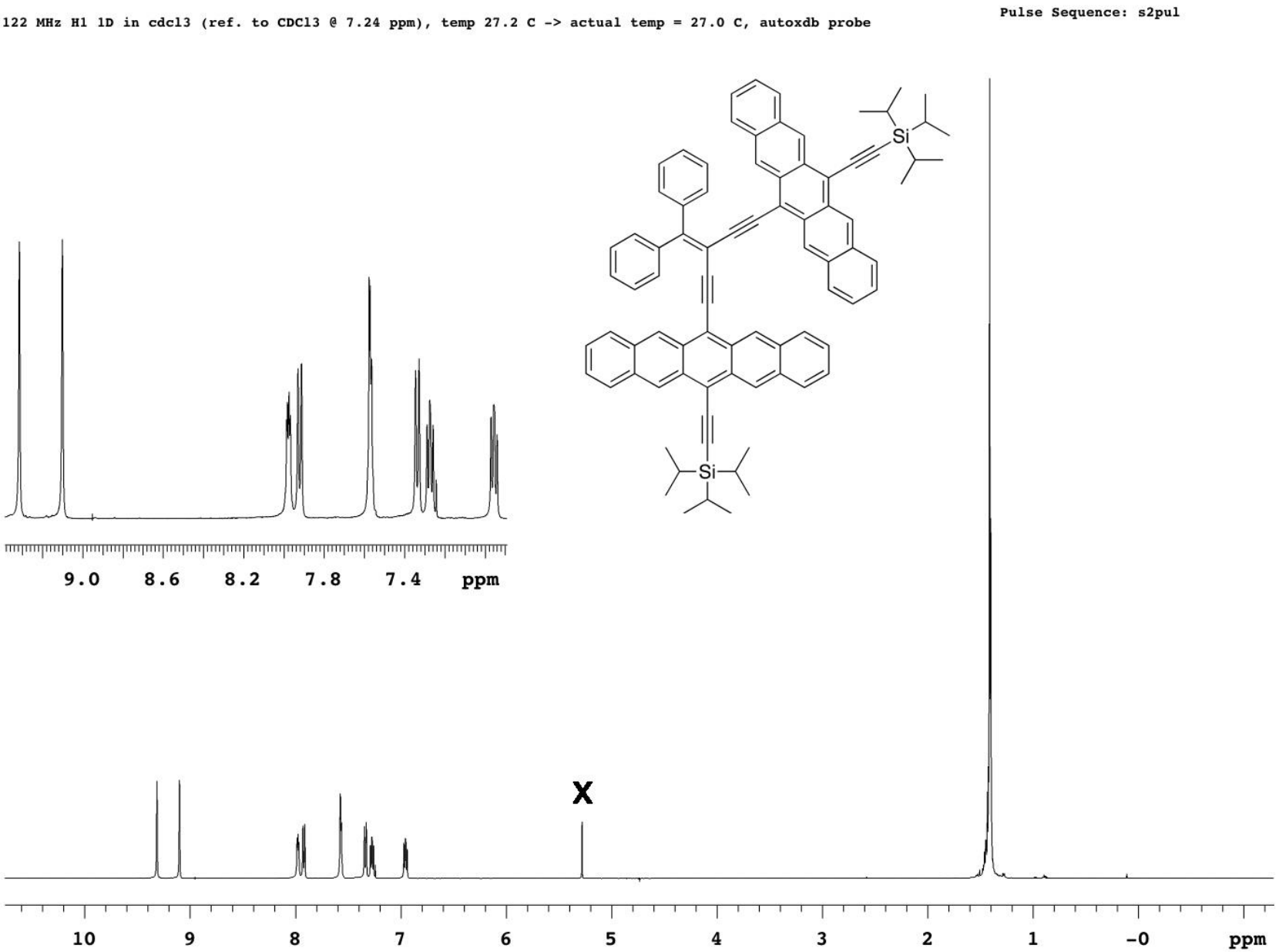

Figure S3: ^{1}H NMR (500 MHz) spectrum of **XC2** in $CDCl_3$ (**x** = CH_2Cl_2).

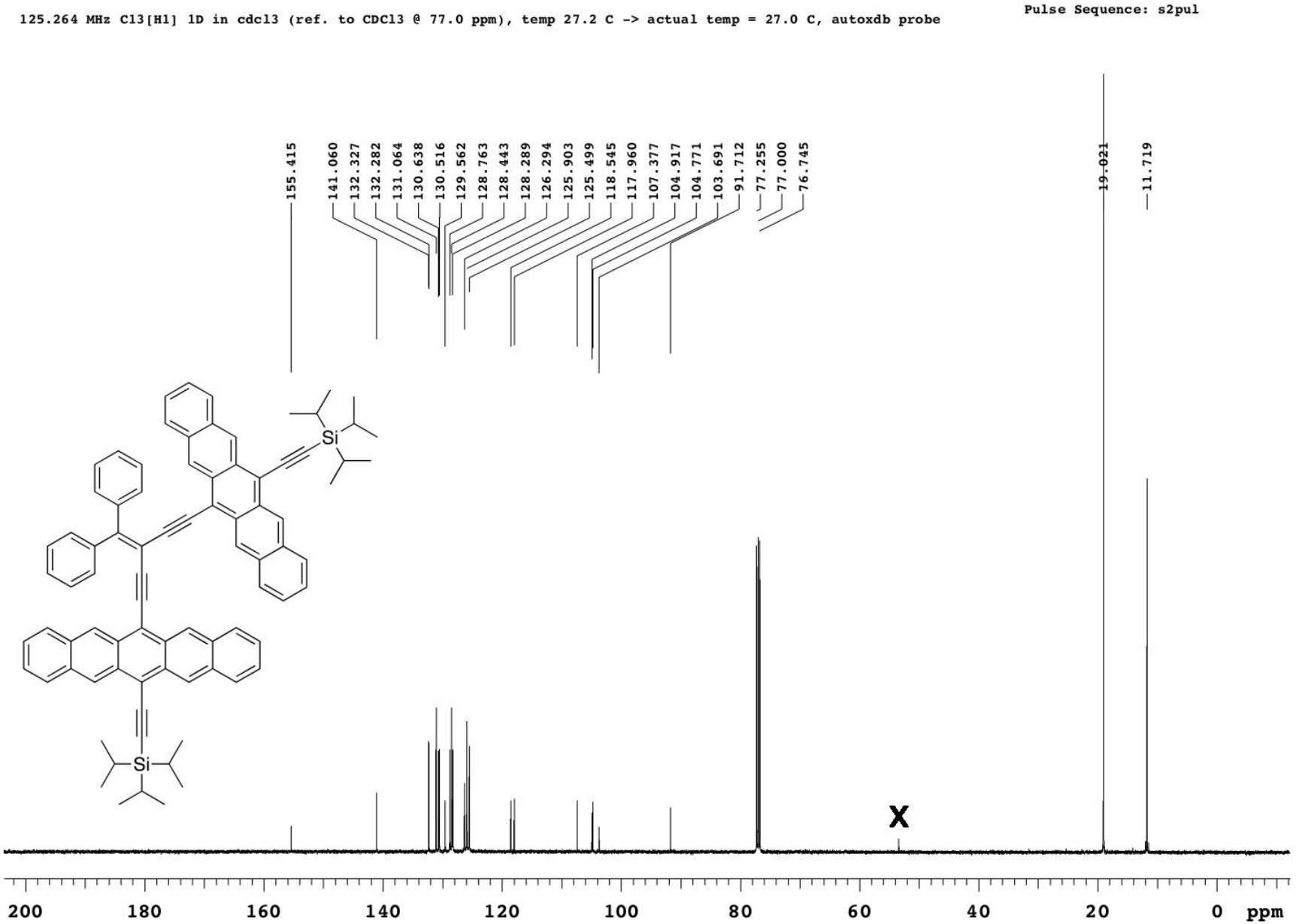

Figure S4: ^{13}C NMR (500 MHz) spectrum of **XC2** in $CDCl_3$ (**x** = CH_2Cl_2).

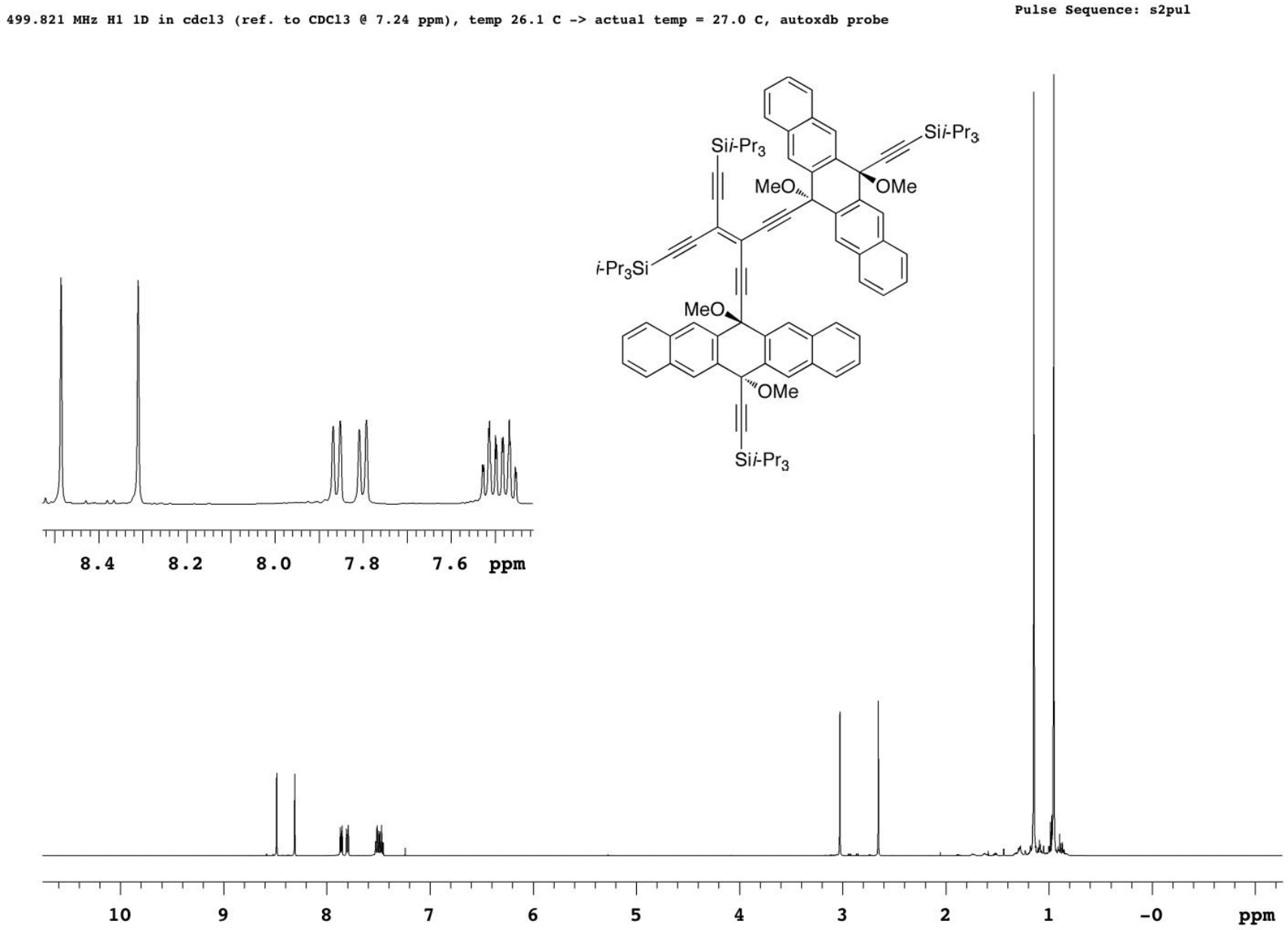

Figure S5: ^{1}H NMR (500 MHz) spectrum of **4** in $CDCl_3$.

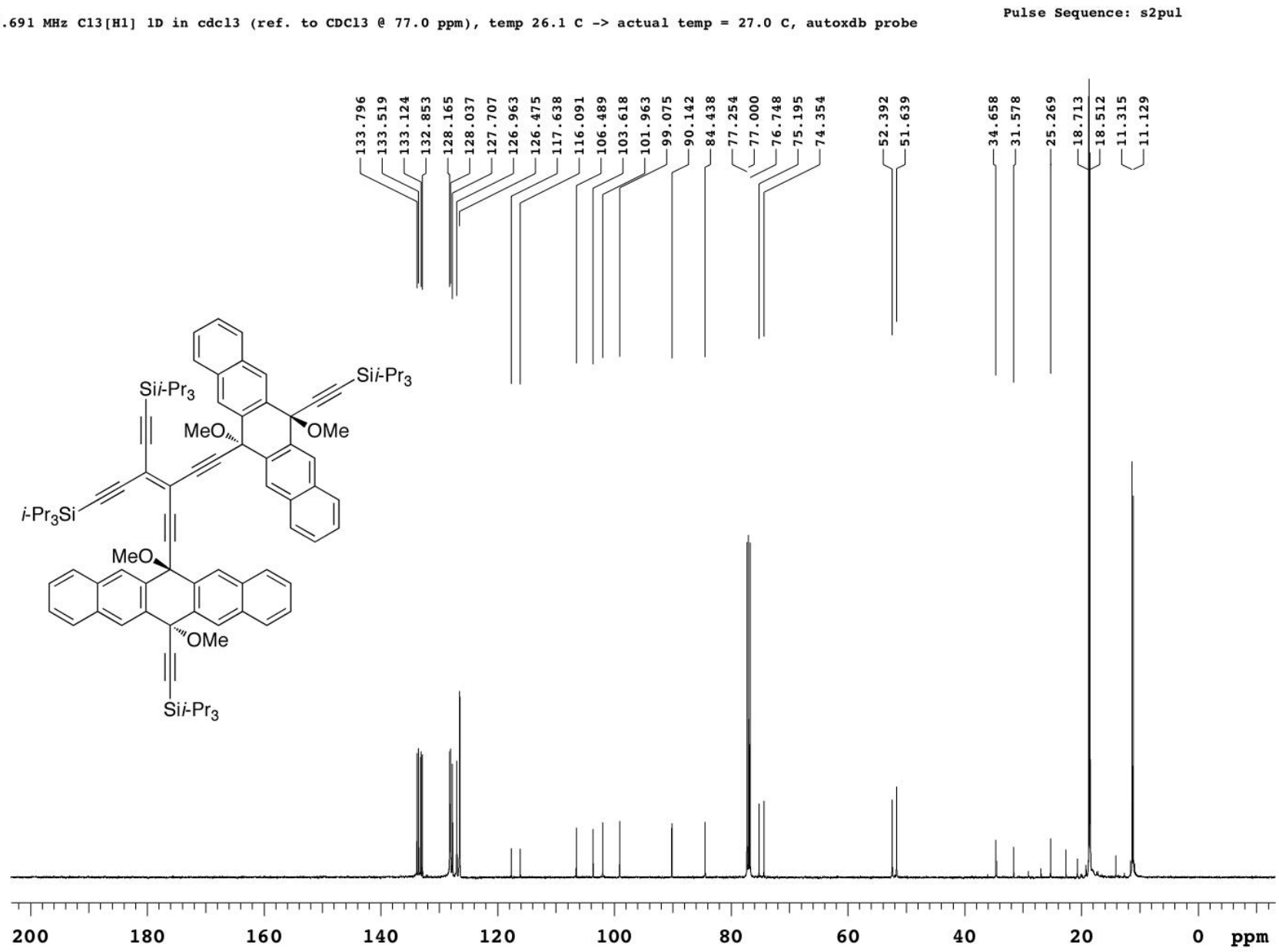

Figure S6: ^{13}C NMR (500 MHz) spectrum of **4** in $CDCl_3$.

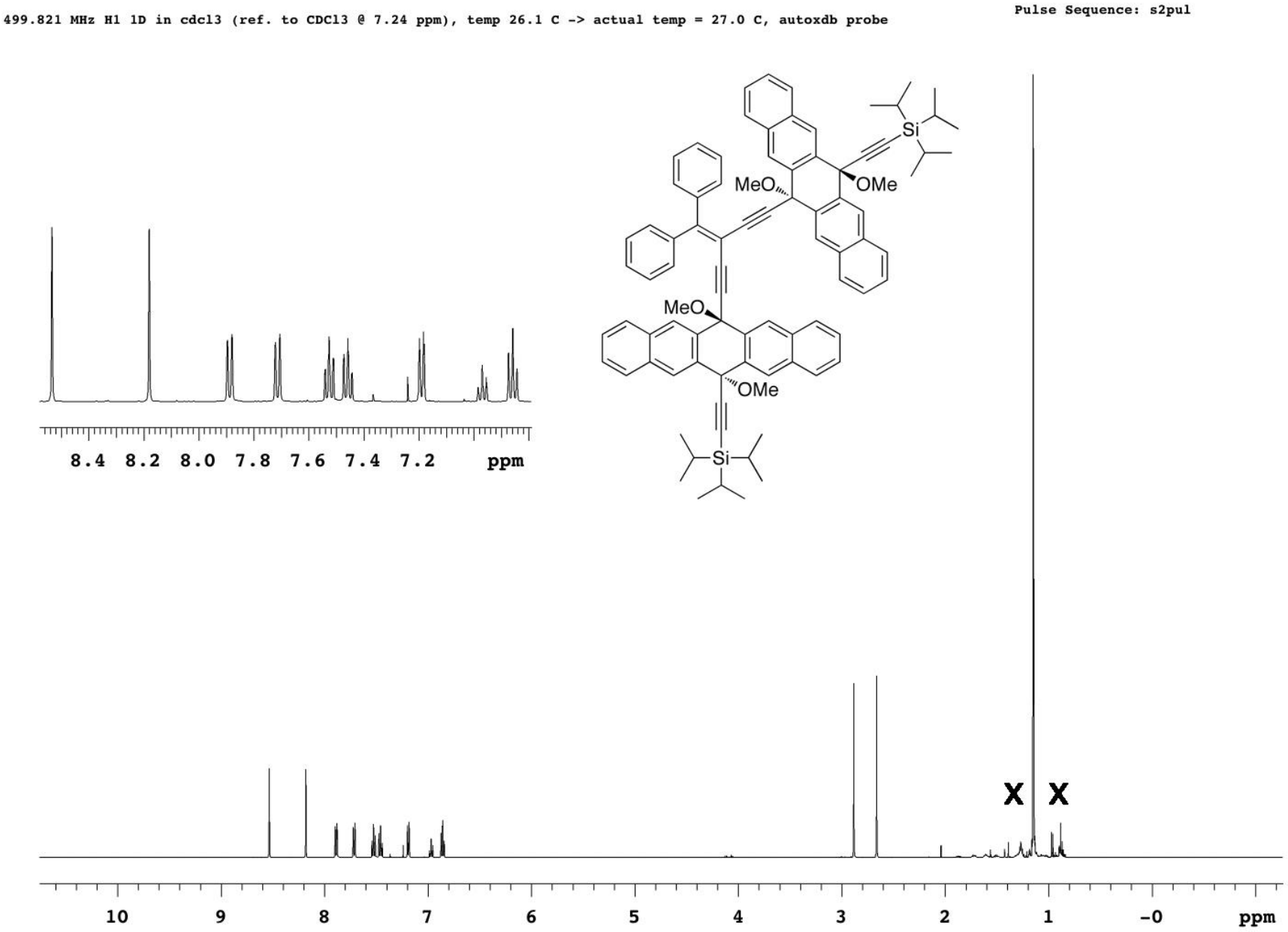

Figure S7: ^{1}H NMR (500 MHz) spectrum of **5** in $CDCl_3$ (**x** = hexanes).

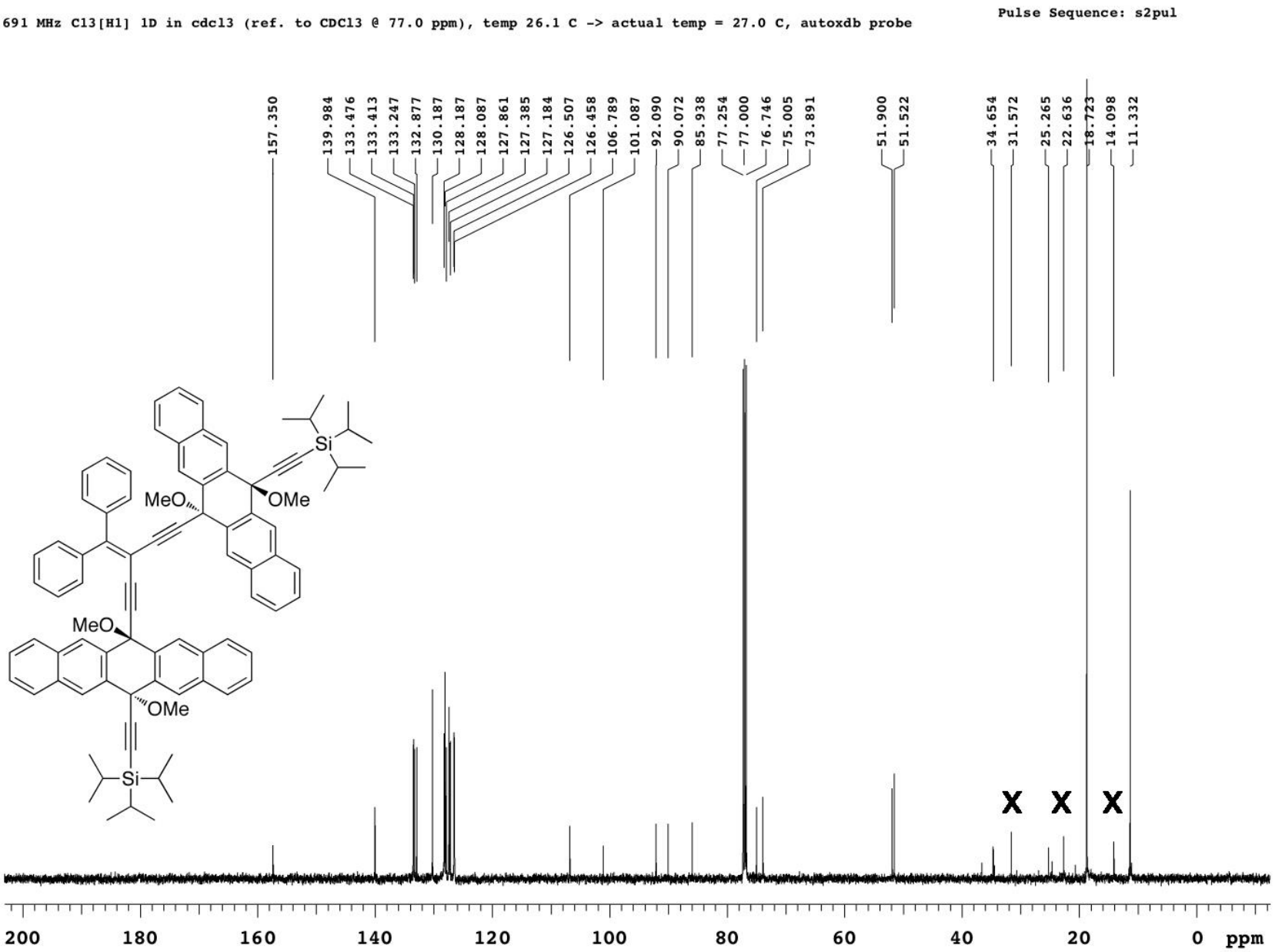

Figure S8: ^{13}C NMR (500 MHz) spectrum of **5** in $CDCl_3$ (**x** = hexanes).

Photophysics

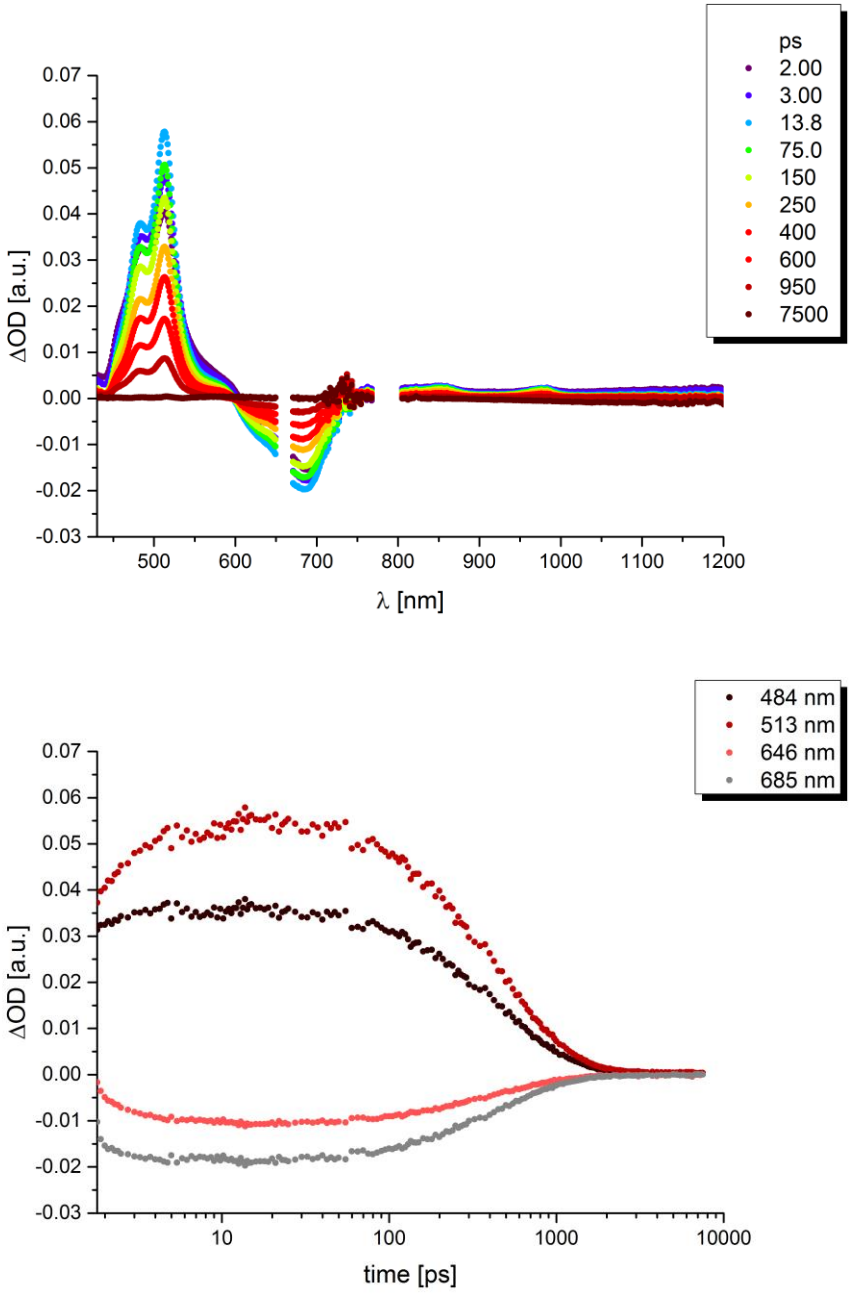

Figure S9: ***Top***: Differential absorption changes (visible and near-infrared) obtained upon femtosecond pump probe experiments (656 nm) of **XC1** (5 x 10^{-5} M) in argon-saturated benzonitrile at room temperature with several time delays between 2.00 and 7500 ps. ***Bottom***: Time absorption profiles of the spectra shown in the upper part at 484 nm (black), 513 nm (red), 646 nm (orange), and 685 nm (gray) illustrating the dynamics of the singlet excited state formation followed by the singlet to triplet transformation in the form of singlet fission and triplet-triplet annihilation.

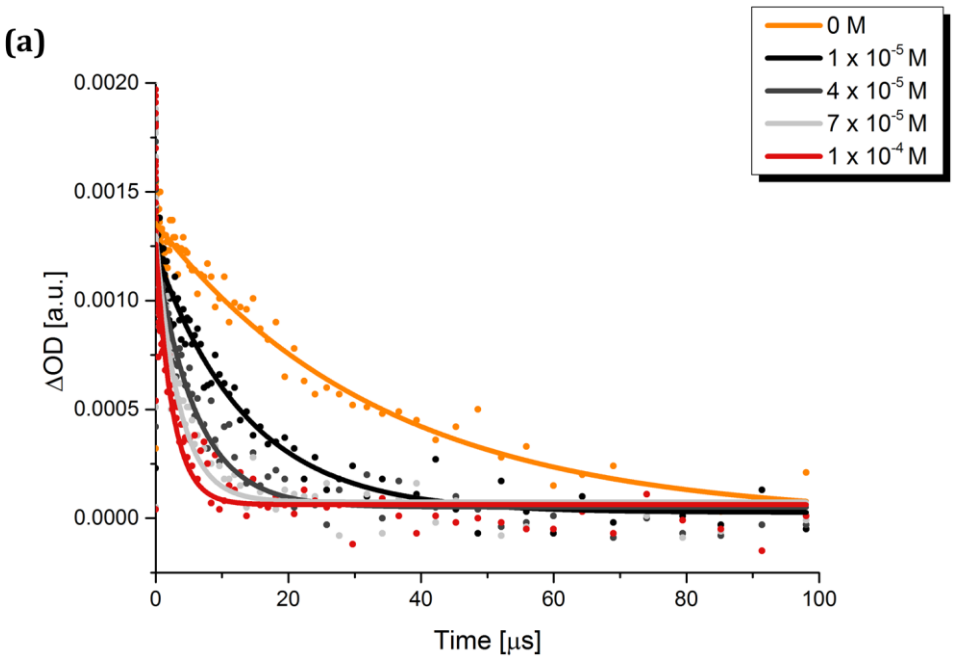
(a)
0 M
1 x 10-5 M
4 x 10-5 M
7 x 10-5 M
1 x 10-4 M
ΔOD [a.u.]
0.0020
0.0015
0.0010
0.0005
0.0000
0
20
40
60
80
100
Time [μs]

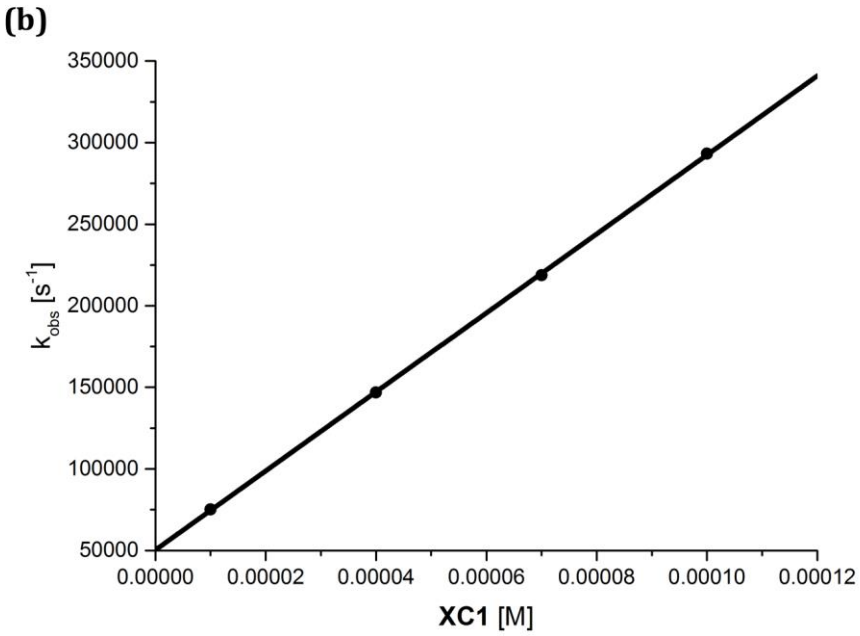
(b)
kobs [s-1]
350000
300000
250000
200000
150000
100000
50000
0.00000
0.00002
0.00004
0.00006
0.00008
0.00010
0.00012
XC1 [M]

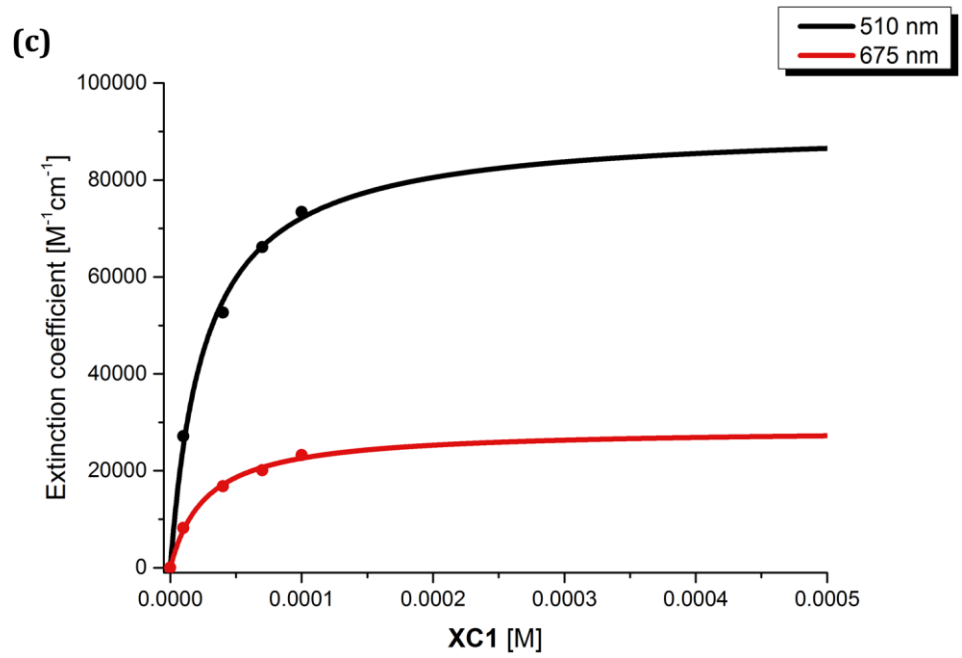

Figure S10: Triplet-triplet sensitization of pentacene dimer **XC1**. (a) Time absorption profiles of the spectra for C_{60} derivative **6** (8.0×10^{-5} M) and variable concentrations of **XC1** (0 – 1.0×10^{-4} M) at 745 nm. (b) Plot of the pseudo-first-order rate constant versus **XC1** concentration in argon-saturated toluene at room temperature to calculate the rate constant for triplet-triplet sensitization. (c) Plot of the calculated extinction coefficient versus **XC1** concentration in argon-saturated toluene at room temperature.

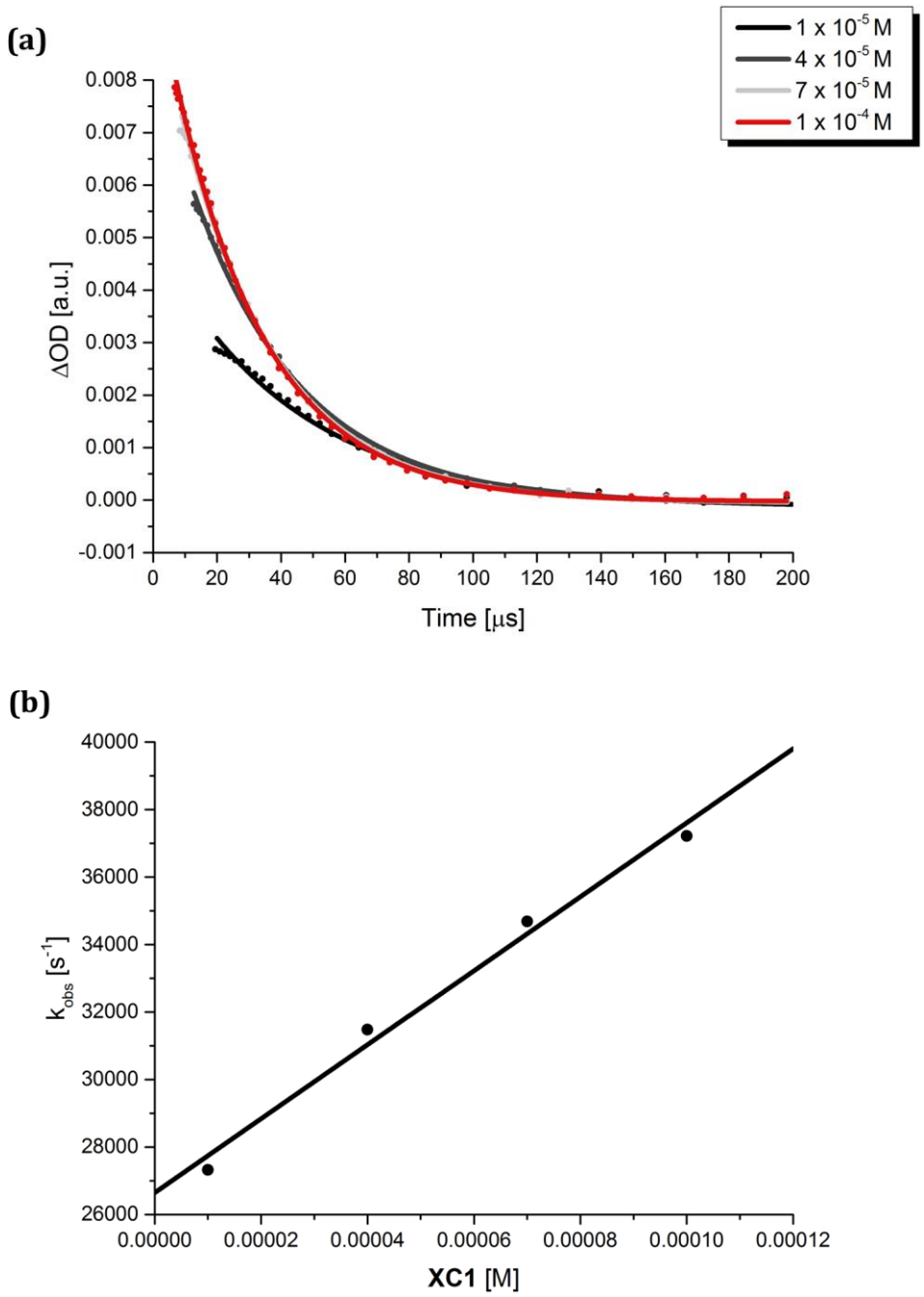

Figure S11: Triplet-triplet annihilation in pentacene dimer **XC1**. (a) Time absorption profiles of the spectra for C_{60} derivative **6** (8.0 x 10^{-5} M) and variable concentrations of **XC1** (1.0 x 10^{-5} – 1.0 x 10^{-4} M) at 510 nm. (b) Plot of the pseudo-first-order rate constant versus **XC1** concentration in argon-saturated toluene at room temperature to calculate the rate constant for triplet-triplet annihilation.

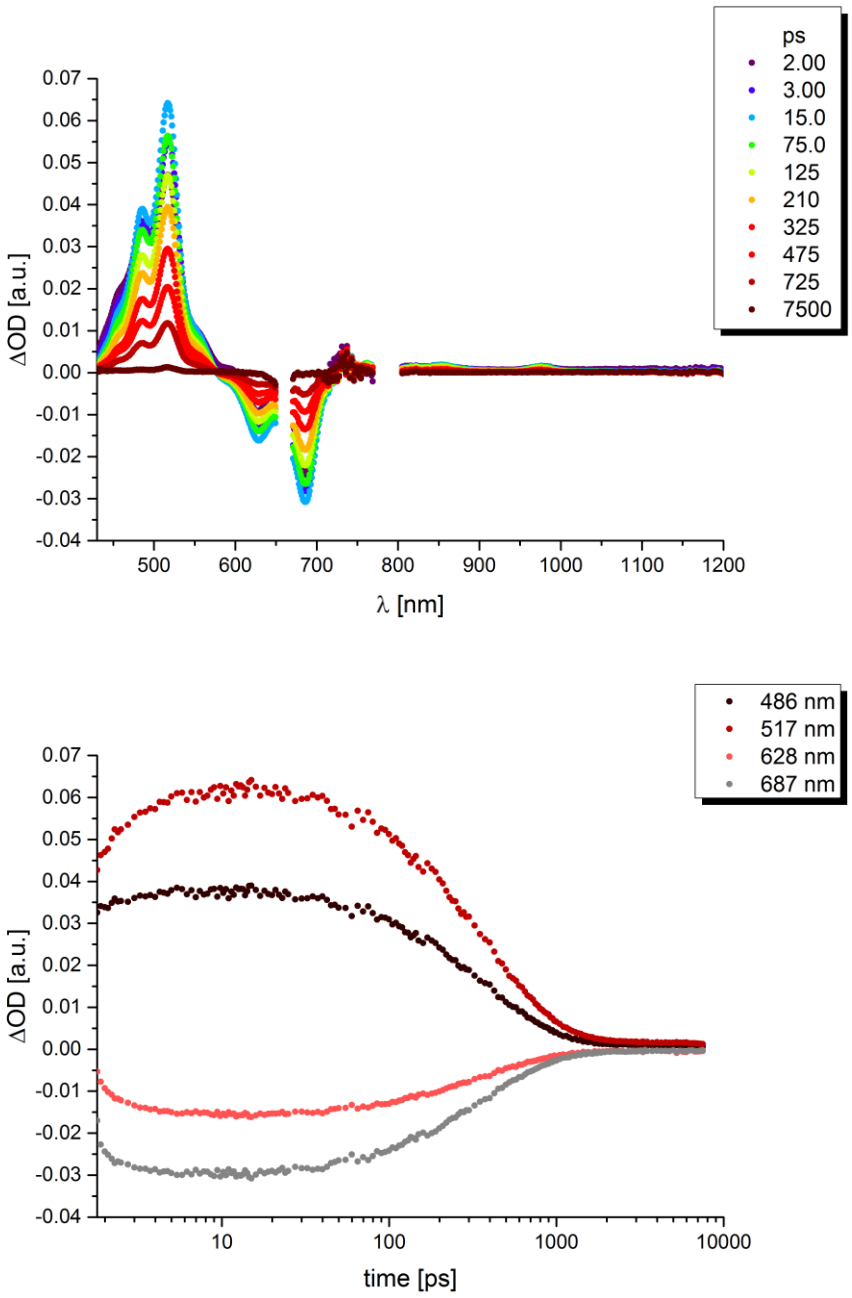

Figure S12: ***Top***: Differential absorption changes (visible and near-infrared) obtained upon femtosecond pump probe experiments (656 nm) of **XC2** (5 x 10^{-5} M) in argon-saturated benzonitrile at room temperature with several time delays between 2.00 and 7500 ps. ***Bottom***: Time absorption profiles of the spectra shown in the upper part at 486 nm (black), 517 nm (red), 628 nm (orange), and 687 nm (gray) illustrating the dynamics of the singlet excited state formation followed by the singlet to triplet transformation in the form of singlet fission and triplet-triplet annihilation.

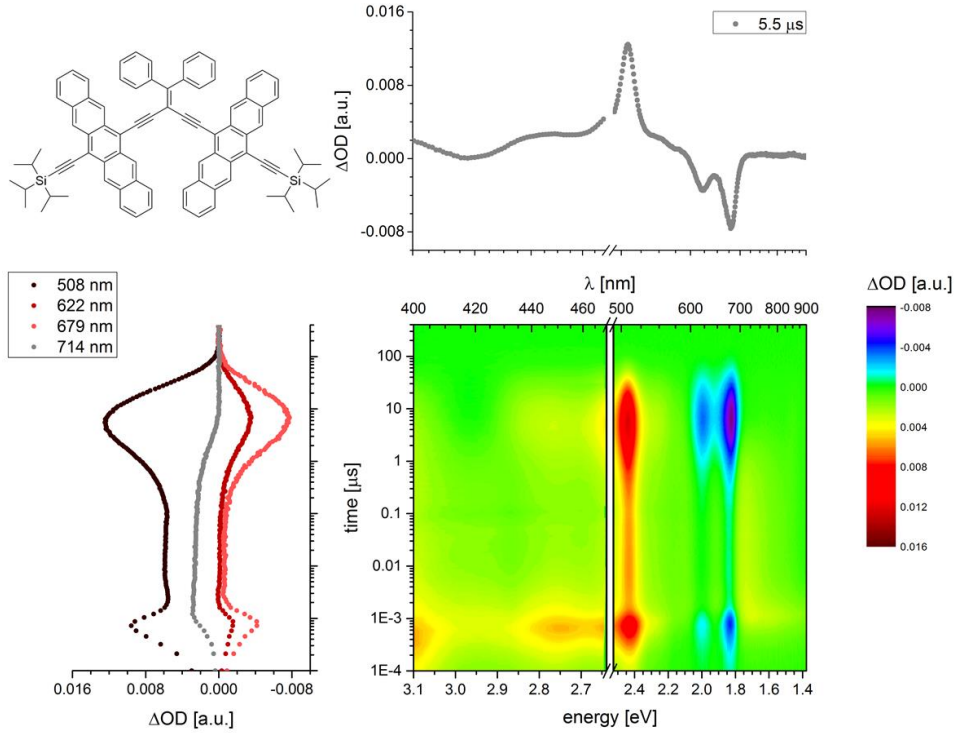

Figure S13: ***Upper left***: Chemical structure of **XC2**. ***Upper right***: Differential absorption spectrum (visible and near-infrared) of the spectra shown in the lower right with a time delay of 5.5 µs representing the triplet excited state of **XC2**. ***Lower left***: Time absorption profiles of the spectra shown in the lower right at 508 nm (black), 622 nm (red), 679 nm (orange), and 714 nm (gray), illustrating the dynamics of the **6** singlet excited state formation followed by the intersystem crossing to the corresponding **6** triplet excited state and transduction of triplet excited state energy to **XC2**. ***Lower right***: Differential absorption changes (visible and near-infrared) obtained upon femtosecond pump probe experiments (480 nm) of **6** (8.0×10^{-5} M) and **XC2** (1.0×10^{-4} M) in argon-saturated toluene at room temperature with several time delays between 0 and 400 µs.

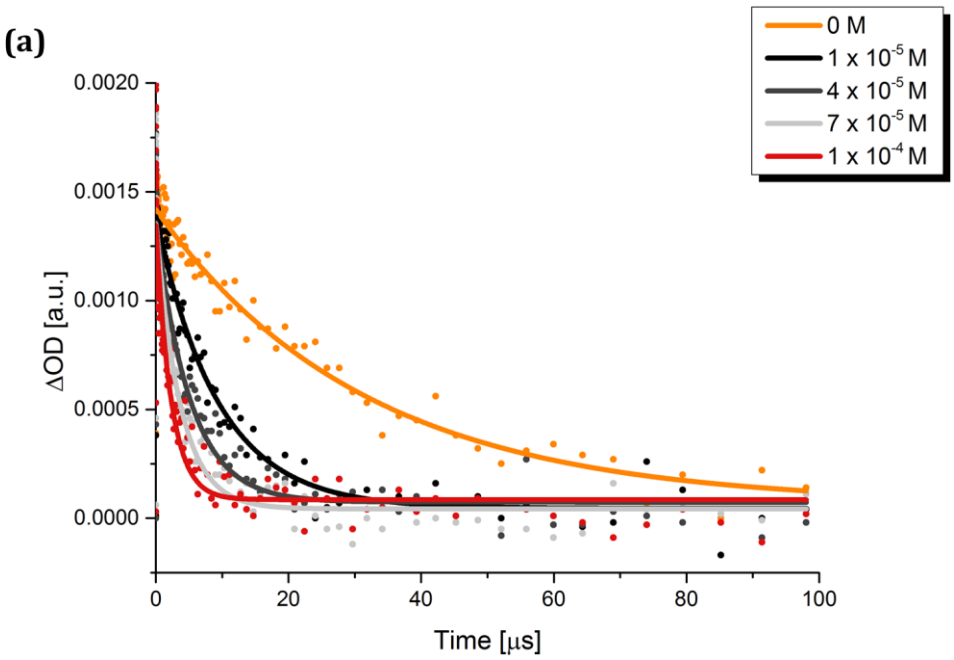
(a)
0 M
1 x 10-5 M
4 x 10-5 M
7 x 10-5 M
1 x 10-4 M
ΔOD [a.u.]
0.0020
0.0015
0.0010
0.0005
0.0000
0
20
40
60
80
100
Time [μs]

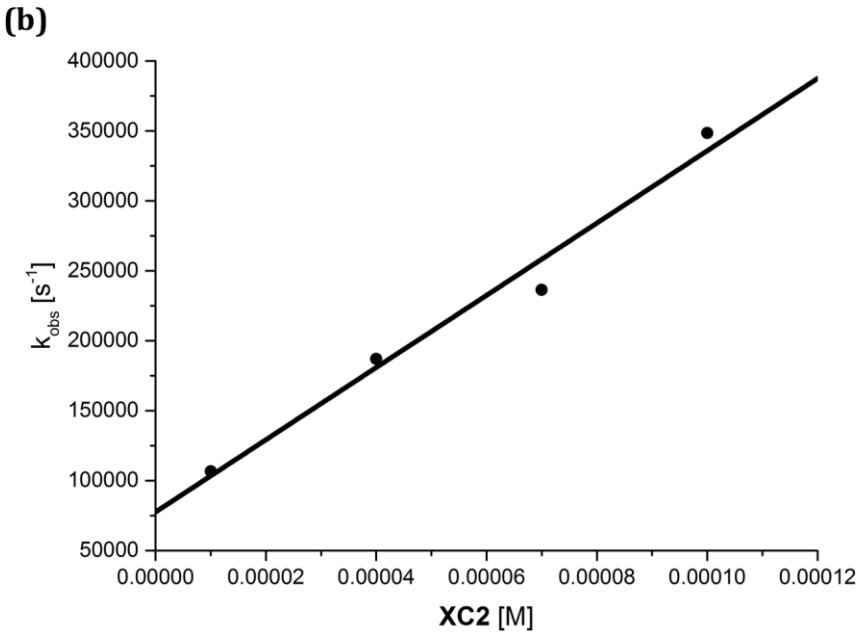
(b)
kobs [s-1]
400000
350000
300000
250000
200000
150000
100000
50000
0.00000
0.00002
0.00004
0.00006
0.00008
0.00010
0.00012
XC2 [M]

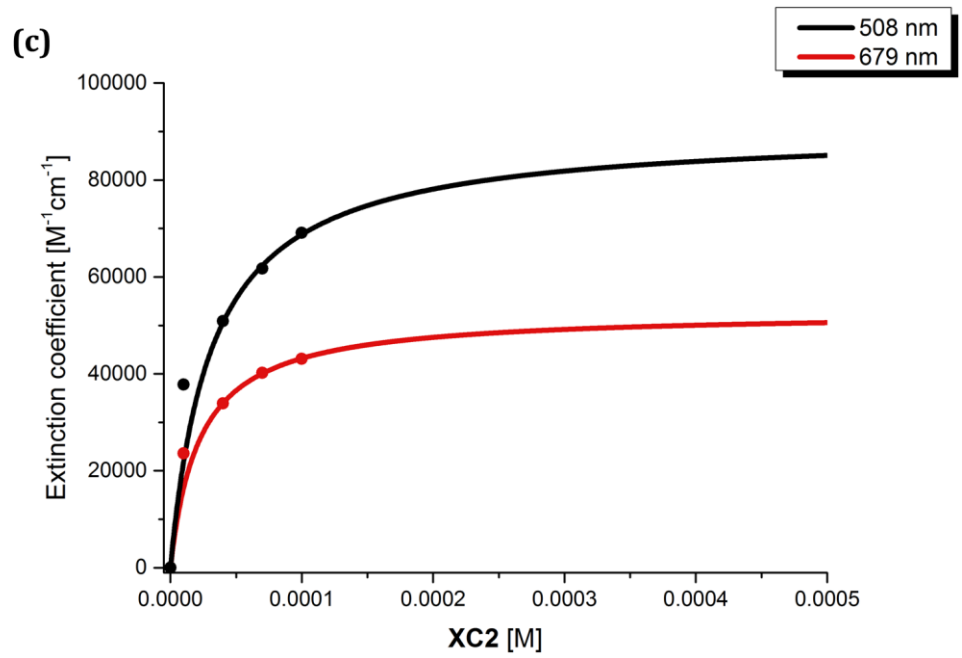

Figure S14: Triplet-triplet sensitization of pentacene dimer **XC2**. (a) Time absorption profiles of the spectra for C_{60} derivative **6** (8.0×10^{-5} M) and variable concentrations of **XC2** (0 – 1.0×10^{-4} M) at 740 nm. (b) Plot of the pseudo-first-order rate constant versus **XC2** concentration in argon-saturated toluene at room temperature to calculate the rate constant for triplet-triplet sensitization. (c) Plot of the calculated extinction coefficient versus **XC2** concentration in argon-saturated toluene at room temperature.

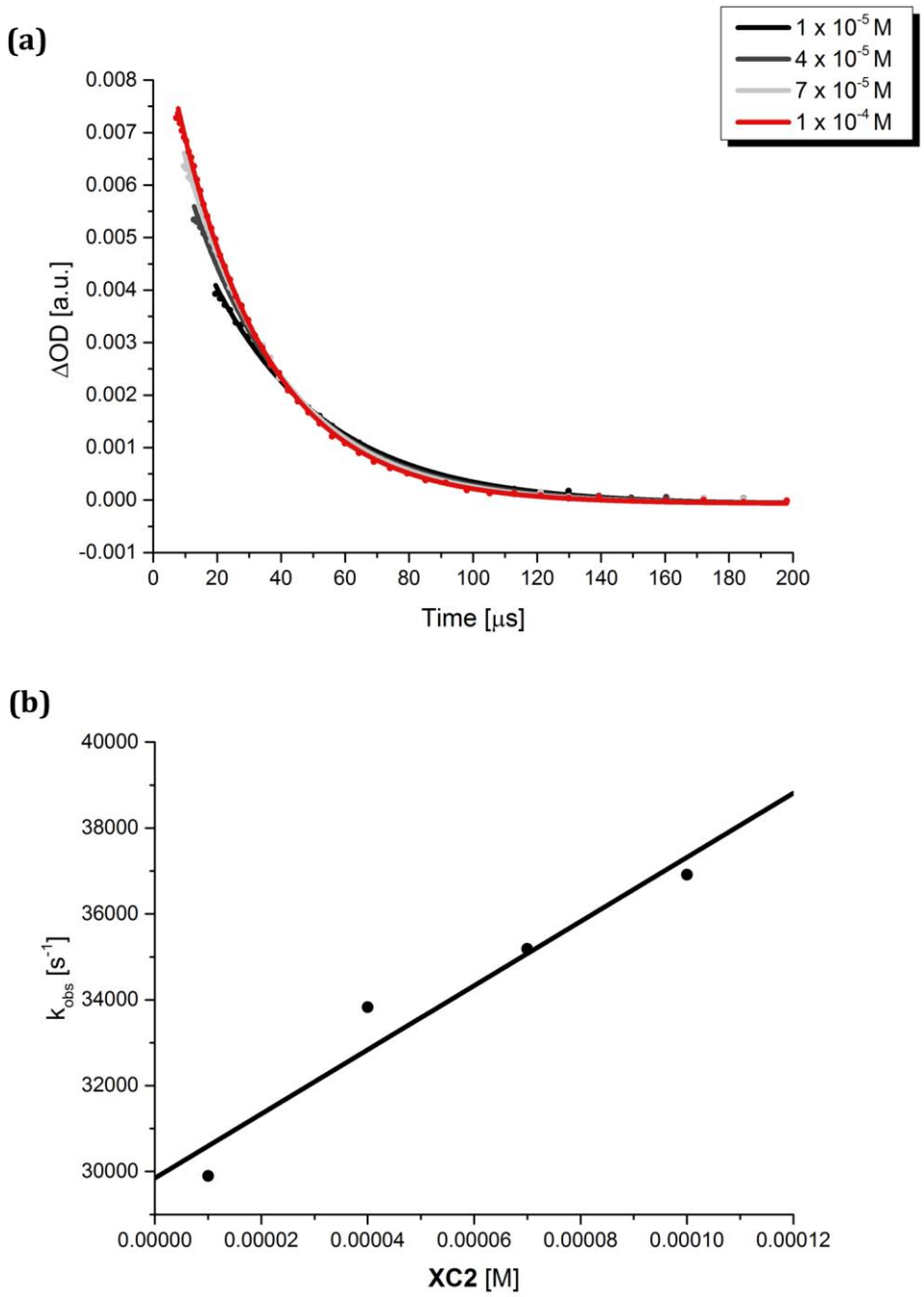

Figure S15: Triplet-triplet annihilation in pentacene dimer **XC2**. (a) Time absorption profiles of the spectra for C_{60} derivative **6** (8.0×10^{-5} M) and variable concentrations of **XC2** (1.0×10^{-5} – 1.0×10^{-4} M) at 508 nm. (b) Plot of the pseudo-first-order rate constant versus **XC2** concentration in argon-saturated toluene at room temperature to calculate the rate constant for triplet-triplet annihilation.

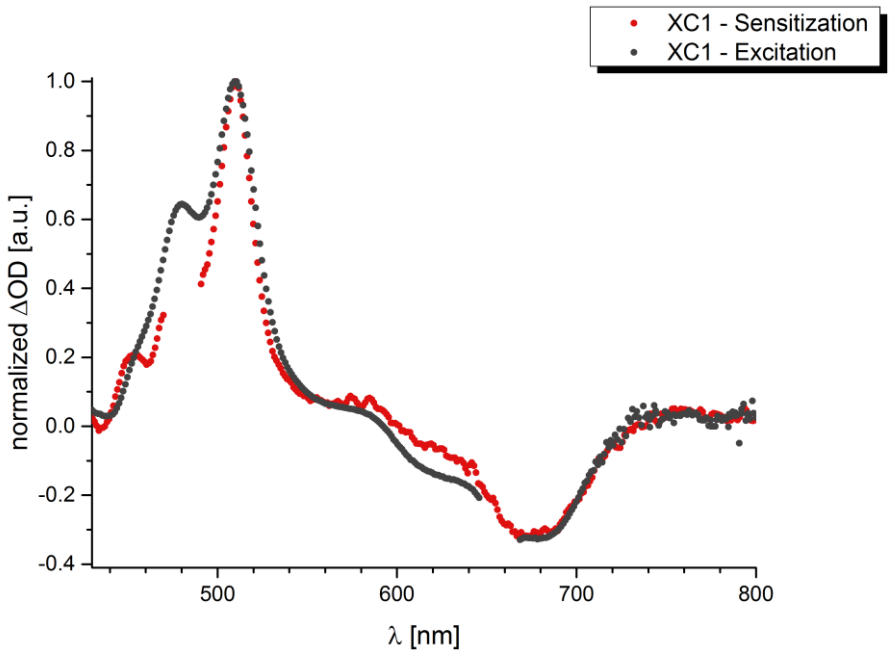

Figure S16: Differential absorption spectra of the triplet excited state of **XC1** obtained upon femtosecond pump probe experiments via sensitization (red; excitation at 480 nm; **6** (8.0×10^{-5} M) and **XC1** (1.0×10^{-4} M)) and direct excitation (gray, excitation at 656 nm, **XC1** (5.0×10^{-5} M)) in toluene.

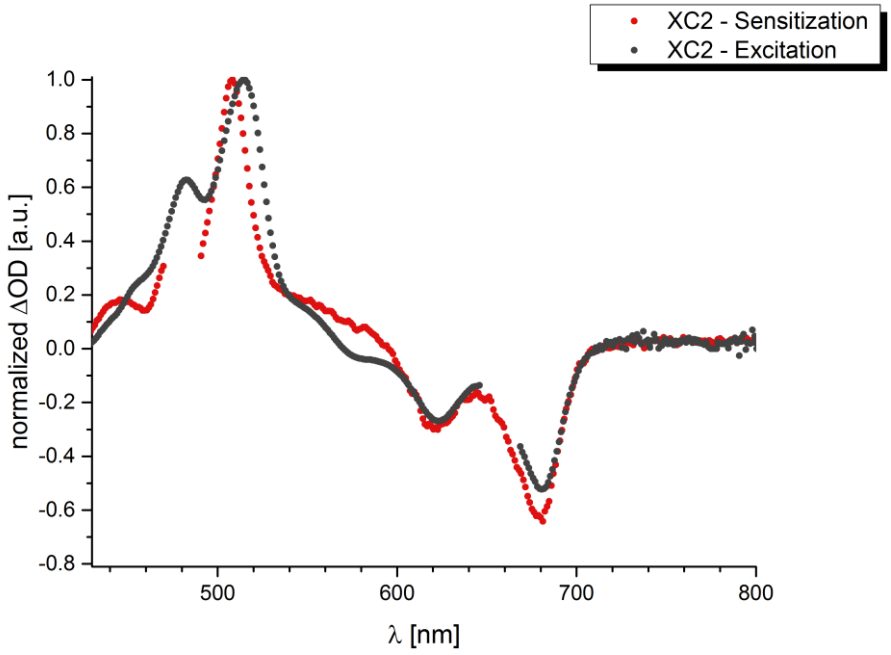

Figure S17: Differential absorption spectra of the triplet excited state of **XC2** obtained upon femtosecond pump probe experiments via sensitization (red; excitation at 480 nm; **6** (8.0×10^{-5} M) and **XC2** (1.0×10^{-4} M)) and direct excitation (gray, excitation at 656 nm, **XC2** (5.0×10^{-5} M)) in toluene.

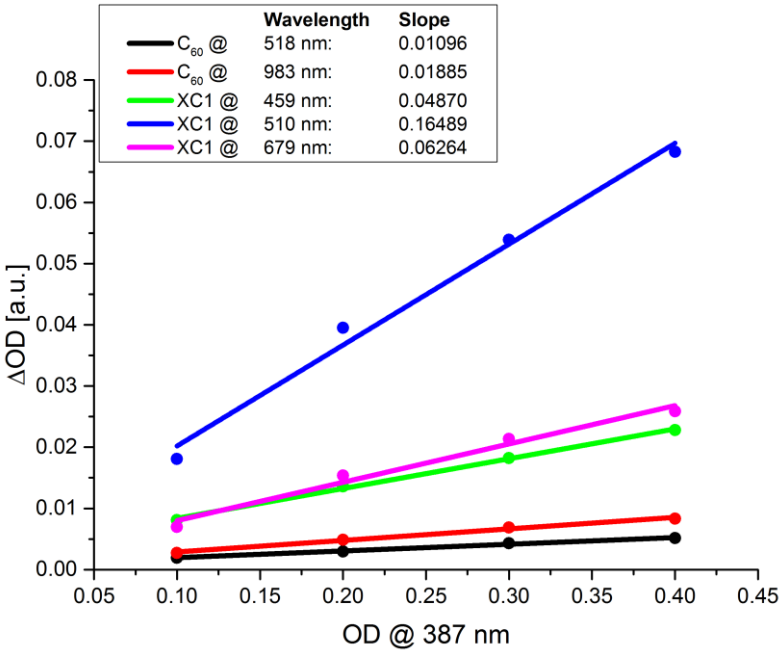
Wavelength Slope
C60 @ 518 nm: 0.01096
C60 @ 983 nm: 0.01885
XC1 @ 459 nm: 0.04870
XC1 @ 510 nm: 0.16489
XC1 @ 679 nm: 0.06264
ΔOD [a.u.]
OD @ 387 nm

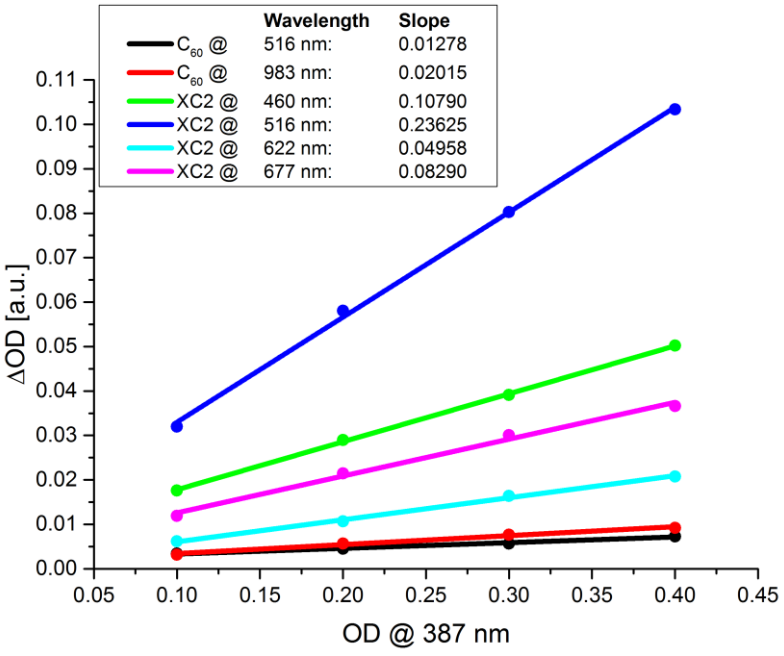
Wavelength Slope
C60 @ 516 nm: 0.01278
C60 @ 983 nm: 0.02015
XC2 @ 460 nm: 0.10790
XC2 @ 516 nm: 0.23625
XC2 @ 622 nm: 0.04958
XC2 @ 677 nm: 0.08290
ΔOD [a.u.]
OD @ 387 nm

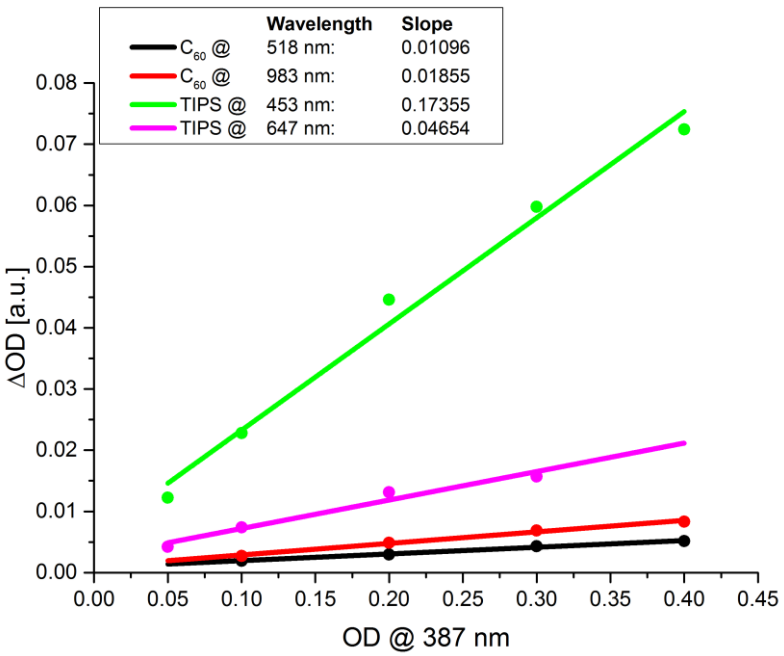

Figure S18: Intensities of the C_{60}, **XC1**, **XC2**, and TIPS Pentacene **7** singlet and triplet excited state markers plotted as a function of absorptivities (OD 0.05 – 0.40). The gradients (slope) for each respective wavelength are given in the legend.

Calculation details

Due to the size of the systems investigated in this work and in order to keep the computational requirements tractable, the isopropyl groups of **XC1** and **XC2** were modeled by methyl groups. Furthermore, we have employed a valence double ζ (DZV) basis set[7] for excited state calculations. To assess the reliability of the DZV basis set, we compared the six roots with equal weights state averaged SA6-CASSCF excitation energies obtained by using DZV and the Dunning´s correlation consistent polarized valence double ζ (cc-pVDZ) basis sets.[8] The results of these calculations are tabulated in Table S1. From Table S1, it can be seen that the excitation energies from the DZV basis set are in good accordance with the results obtained using the cc-pVDZ basis set.

Table S1: Comparison of the SA6-CASSCF excitation energies of **XC1** and **XC2** obtained with DZV and cc-pVDZ basis sets.

State	**XC1**		**XC2**	
	DZV	cc-pVDZ	DZV	cc-pVDZ
S_1	2.65	2.62	2.69	2.64
S_2	3.26	3.16	3.34	3.17
S_3	3.46	3.37	3.50	3.34
S_4	4.13	4.11	4.18	4.11
S_5	4.20	4.16	4.22	4.23

For all systems investigated, the canonical orbitals obtained at the CASSCF level are delocalized over the two pentacene units. To facilitate electronic state characterization in terms of molecular orbitals maximally localized in each pentacene unit, we have performed a unitary transformation of the optimized active space orbitals, which are obtained in the CASSCF calculations. The characterization of the electronic states as multi-excitonic (ME), local excitation (LE), and charge transfer (CT) states is shown in Figs. S19 and S20 for **XC1** and **XC2**, respectively.

To get insight into the SF mechanism, we have investigated the diabatic electronic states relevant for the process and their interstate couplings.[9] These diabatic electronic states can be obtained by a suitable unitary transformation of the adiabatic electronic states. Among the different

methods available, in this work we have employed the four-fold-way diabatization method of Truhlar and co-workers.[10,11] In the following, first we will briefly describe the procedure of the four-fold-way and then we will present our results. The four-fold-way is based on the configurational uniformity concept proposed by Ruedenberg and co-workers.[12,13] In this work, the adiabatic wavefunctions used in the diabatization process have been built using all configuration state functions (CSFs) whose coefficients are more than 0.20 in any of the adiabatic electronic states considered. The adiabatic (canonical) molecular orbitals of the active space that define the CSFs are then rotated such that they satisfy the so called three-fold density criterion and MORMO conditions to form diabatic molecular orbitals (DMOs).[10,11] The adiabatic states are then re-expressed by CSFs defined by DMOs and are transformed to diabatic states by applying a unitary transformation.

The six low-lying adiabatic electronic states of **XC1** and **XC2** at their respective optimized structure (see Table 2 of the article) were included in the diabatization process. We have selected 12 and 15 CSFs whose coefficients are more than 0.20 for **XC1** and **XC2,** respectively. Maximally localized DMOs were obtained in the calculations. The weights of the dominant CSFs obtained from the DMOs in the adiabatic states S_0, S_1, S_2, S_3, S_4 and S_5 for **XC1** were 99.1%, 94.4%, 99.5%, 99.4%, 95.1%, and 94.8%, respectively. Similarly for **XC2**, these weights were 99.7%, 100.0%, 93.9%, 96.3%, 99.8%, and 99.7%. It can be seen that the contributions from the dominant CSFs are ~94% or more for both **XC1** and **XC2**.

The adiabatic electronic states (S_0, S_1, S_2, S_3, S_4 and S_5) are the linear combination of the diabatic states ($|S_0S_0\rangle$, $|T_1T_1\rangle$, $|S_1S_0\rangle$, $|S_0S_1\rangle$, |CA> and |AC>). The adiabatic electronic states of **XC1** and **XC2** in terms of the respective diabatic electronic states are presented in equations (1) and (2), respectively.

$$\begin{pmatrix} |S_0> \\ |S_1> \\ |S_2> \\ |S_3> \\ |S_4> \\ |S_5> \end{pmatrix} = \begin{pmatrix} 0.99 & 0.00 & -0.13 & -0.06 & -0.03 & 0.00 \\ -0.02 & -0.97 & -0.15 & -0.08 & 0.17 & 0.04 \\ 0.12 & -0.21 & 0.90 & 0.11 & -0.31 & -0.12 \\ 0.04 & -0.04 & -0.10 & 0.98 & 0.14 & -0.07 \\ 0.05 & 0.10 & 0.24 & -0.13 & 0.81 & -0.51 \\ -0.05 & -0.07 & -0.28 & -0.02 & -0.45 & -0.84 \end{pmatrix} \begin{pmatrix} |S_0S_0> \\ |T_1T_1> \\ |S_1S_0> \\ |S_0S_1> \\ |CA> \\ |AC> \end{pmatrix} \quad (1)$$

$$\begin{pmatrix} |S_0> \\ |S_1> \\ |S_2> \\ |S_3> \\ |S_4> \\ |S_5> \end{pmatrix} = \begin{pmatrix} 0.99 & 0.01 & 0.07 & -0.07 & 0.07 & 0.06 \\ -0.02 & 1.00 & 0.03 & -0.03 & 0.08 & -0.02 \\ -0.13 & -0.07 & 0.65 & -0.38 & 0.60 & 0.37 \\ 0.02 & 0.01 & 0.58 & 0.75 & -0.09 & -0.08 \\ 0.00 & 0.00 & 0.48 & -0.52 & -0.64 & -0.52 \\ -0.01 & 0.06 & 0.12 & -0.10 & -0.46 & 0.75 \end{pmatrix} \begin{pmatrix} |S_0S_0> \\ |T_1T_1> \\ |S_1S_0> \\ |S_0S_1> \\ |CA> \\ |AC> \end{pmatrix} \quad (2)$$

State	Orbital transition	Weight	Character
S_1	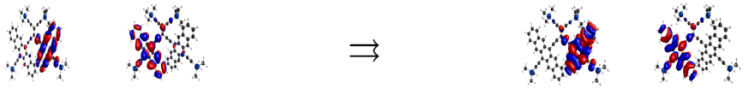	0.75	ME
S_2	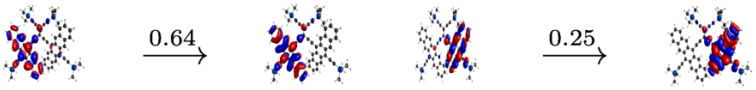	0.89	LE
S_3	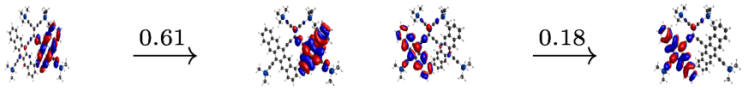	0.79	LE
S_4	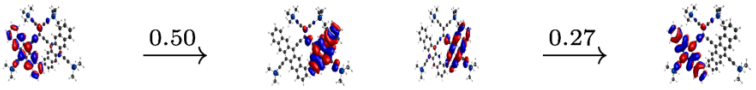	0.77	CT
S_5	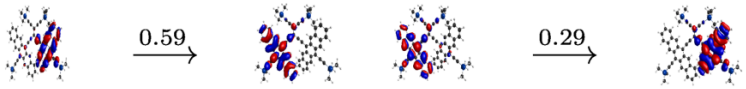	0.88	CT

Figure S19: Characterization of the adiabatic excited electronic states of **XC1** in terms of the electron excitations involving localized CASSCF molecular orbitals.[a, b, c]

[a] Double arrows represent double excitations and single arrows represent single excitations.
[b] The number on each arrow is the weight of the particular excitation in the wavefunction of the adiabatic state.
[c] Character of excited state: ME=multiexcitonic state, LE=excited states that correlate with the plus and minus combinations of locally excited states of both pentacene monomers, CT=charge transfer states.

State	Orbital transition	Weight	Character
S_1	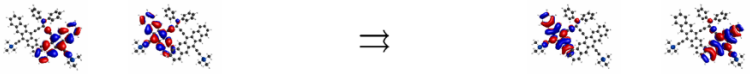	0.99	ME
S_2	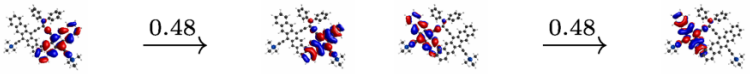	0.96	LE
S_3	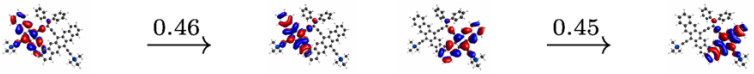	0.91	LE
S_4		0.94	CT
S_5	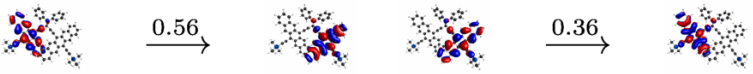	0.92	CT

Figure S20: Characterization of the adiabatic excited electronic states of **XC2** in terms of electron excitations involving localized CASSCF molecular orbitals.[a, b, c]

[a] Double arrows represent double excitations and single arrows represent single excitations.
[b] The number on each arrow is the weight of the particular excitation in the wavefunction of the adiabatic state.
[c] Character of excited state: ME=multiexcitonic state, LE=excited states that correlate with the plus and minus combinations of locally excited states of both pentacene monomers, CT=charge transfer states.

Cartesian Coordinates

XC1 Cartesian coordinates:

C	-5.43606	1.82479	2.35673
C	-4.31601	1.49244	1.61413
C	-3.44706	2.47032	1.10333
C	-3.72302	3.86196	1.37646
C	-4.86950	4.18782	2.12334
C	-5.72749	3.21601	2.61166
C	-2.30488	2.11679	0.34009
C	-2.83573	4.86063	0.89921
C	-1.69080	4.50673	0.13992
C	-1.43129	3.11679	-0.15888
C	-0.31244	2.78919	-0.94299
H	-0.12887	1.74890	-1.18070
C	0.56635	3.75310	-1.40762
C	0.32885	5.13897	-1.07900
C	-0.78807	5.47639	-0.33155
H	-4.10454	0.45032	1.41044
H	-5.08136	5.23095	2.32019
H	-0.97546	6.51641	-0.09639
C	1.26625	6.11756	-1.53536
C	1.72148	3.41772	-2.17872
C	2.58866	4.38179	-2.58835
C	2.35802	5.75197	-2.26099
H	1.08820	7.15778	-1.28801
H	3.06391	6.50186	-2.59636
H	3.46845	4.11395	-3.16008
H	1.90146	2.37472	-2.41056
C	-6.89817	3.53949	3.36673
H	-7.11563	4.58353	3.56004
C	-6.32389	0.83154	2.87336
H	-6.09235	-0.21020	2.68684
C	-7.43008	1.18530	3.58166
H	-8.09861	0.42342	3.96344
C	-7.72119	2.56068	3.83214
H	-8.60566	2.81841	4.40174
C	2.98304	-6.04183	-0.49711
C	2.36384	-4.80512	-0.39773
C	3.09944	-3.61841	-0.24854
C	4.54262	-3.69337	-0.21581
C	5.15949	-4.94967	-0.35044
C	4.42523	-6.11600	-0.48499
C	2.45741	-2.35851	-0.10496
C	5.30565	-2.50963	-0.04487

C	4.66555	-1.25862	0.14894
C	3.22199	-1.18350	0.14545
C	2.61121	0.05444	0.40535
H	1.53035	0.10857	0.43496
C	3.35057	1.20252	0.64743
C	4.79216	1.13950	0.58930
C	5.40465	-0.07963	0.35132
H	1.28185	-4.74908	-0.41526
H	6.24055	-5.00200	-0.33311
H	6.48550	-0.13612	0.33036
C	5.53668	2.34341	0.79096
C	2.73244	2.45425	0.94935
C	3.48004	3.57477	1.13736
C	4.90326	3.52034	1.04814
H	6.61810	2.29659	0.73472
H	5.47795	4.42693	1.19317
H	2.99584	4.52127	1.34366
H	1.65279	2.49558	1.00585
C	5.04540	-7.39954	-0.59998
H	6.12806	-7.45071	-0.59693
C	2.23983	-7.25714	-0.59981
H	1.16023	-7.19983	-0.59043
C	2.87042	-8.45853	-0.69963
H	2.29129	-9.37079	-0.77374
C	4.29623	-8.53095	-0.70493
H	4.77723	-9.49774	-0.78910
C	6.71798	-2.58254	-0.04597
C	7.93119	-2.65010	-0.04303
C	-3.09236	6.22019	1.19163
C	-3.31591	7.38566	1.45233
C	-2.03166	0.76030	0.08497
C	-1.80928	-0.41068	-0.12790
C	1.06185	-2.25349	-0.21264
C	-0.13613	-2.09851	-0.32906
C	-1.50081	-1.76276	-0.39715
C	-2.50135	-2.66784	-0.72417
C	-2.21852	-4.00389	-1.08953
C	-3.85586	-2.25891	-0.77016
C	-2.03479	-5.14332	-1.46853
C	-5.01807	-1.91145	-0.83719
Si	9.76316	-2.76728	-0.02318
Si	-3.66611	9.13791	1.86990
Si	-1.84245	-6.82247	-2.18854
Si	-6.75913	-1.36150	-1.06514
C	-2.24277	9.80052	2.89886
H	-1.30111	9.74372	2.34800

H	-2.41489	10.84654	3.16681
H	-2.12626	9.22863	3.82199
C	-3.82756	10.11323	0.27450
H	-4.63867	9.72334	-0.34426
H	-4.03650	11.16570	0.48472
H	-2.90597	10.06229	-0.30990
C	-5.26798	9.19429	2.84752
H	-6.09858	8.79062	2.26397
H	-5.18554	8.60965	3.76668
H	-5.51744	10.22245	3.12302
C	10.40253	-1.77613	1.43671
H	11.49402	-1.81859	1.48553
H	10.10918	-0.72690	1.35647
H	10.00548	-2.16435	2.37716
C	10.23020	-4.57722	0.15151
H	9.82270	-4.99810	1.07348
H	9.84662	-5.16465	-0.68590
H	11.31668	-4.69642	0.17712
C	-0.34314	-6.81483	-3.31659
H	0.56125	-6.49067	-2.80037
H	-0.15965	-7.81403	-3.72083
H	-0.50854	-6.13611	-4.15646
C	-1.66780	-8.07462	-0.79869
H	-1.45195	-9.06688	-1.20442
H	-0.87084	-7.81328	-0.10071
H	-2.59624	-8.13920	-0.22666
C	-3.39052	-7.20015	-3.17975
H	-4.27872	-7.18033	-2.54436
H	-3.53164	-6.46815	-3.97782
H	-3.32132	-8.19149	-3.63613
C	10.42598	-2.06442	-1.63263
H	10.04189	-2.61903	-2.49153
H	10.13536	-1.01819	-1.75204
H	11.51793	-2.11702	-1.65504
C	-7.37923	-2.09736	-2.67736
H	-6.77271	-1.75824	-3.52003
H	-7.33926	-3.18865	-2.65280
H	-8.41470	-1.79879	-2.86266
C	-7.79675	-1.98709	0.36976
H	-7.74348	-3.07480	0.45200
H	-7.46432	-1.55772	1.31634
H	-8.84436	-1.70767	0.22780
C	-6.78902	0.51082	-1.13845
H	-6.43481	0.95099	-0.20508
H	-6.15300	0.88039	-1.94558
H	-7.80666	0.86912	-1.31543

XC2 Cartesian coordinates:

Si	8.59122	-4.42326	0.19603
Si	-8.71674	-4.16557	-0.05249
C	5.57990	-0.05702	-0.07277
C	3.68621	-3.14731	0.92918
H	4.48220	-3.88022	0.89396
C	6.08740	2.65942	-0.71906
C	4.50913	0.91305	-0.07854
C	2.41145	-3.54580	1.29649
C	-4.45814	1.03644	0.12879
C	1.21754	2.21918	0.10097
C	3.18941	0.50483	0.24780
C	4.80238	2.24687	-0.40910
H	3.99978	2.97323	-0.41093
C	2.13292	1.43058	0.18142
C	2.91883	-0.83854	0.62187
C	3.98572	-1.81301	0.60055
C	1.63479	-1.24873	1.02093
H	0.84051	-0.51397	1.05822
C	-7.32425	-2.97270	-0.08448
C	7.15978	1.69128	-0.71396
C	-5.56070	0.10256	0.14157
C	6.38951	4.01855	-1.04447
H	5.58020	4.73934	-1.04232
C	5.30040	-1.40966	0.25099
C	1.35741	-2.56114	1.36638
C	-1.13275	2.23742	-0.08091
C	-3.15338	0.57833	-0.19171
C	6.87951	0.37223	-0.39675
H	7.68151	-0.35488	-0.39402
C	6.34350	-2.36388	0.23317
C	-7.08028	1.91445	0.75152
C	-2.06796	1.47102	-0.14465
C	-4.70579	2.38490	0.43650
H	-3.87959	3.08410	0.42452
C	-4.02707	-1.71771	-0.50194
C	-1.42431	-2.56585	-1.25339
C	7.23913	-3.18492	0.21940
C	2.24411	4.82858	1.15673
H	2.04916	3.99993	1.82296
C	2.09657	-4.90542	1.60802
H	2.88665	-5.64485	1.54764
C	-2.92839	-0.77971	-0.54139
C	-1.65866	-1.23903	-0.93248
H	-0.84064	-0.53153	-0.98195

C	1.30269	5.16166	0.17384
C	-7.48964	4.64414	1.33921
H	-7.67266	5.68687	1.56868
C	-6.84500	0.58137	0.45719
H	-7.67141	-0.11781	0.46570
C	0.05105	-2.98217	1.76451
H	-0.73768	-2.24170	1.80928
C	-5.97570	2.84556	0.74070
C	-0.20404	-4.28737	2.04747
H	-1.20357	-4.59694	2.32610
C	-6.23094	4.21922	1.04469
H	-5.39745	4.91162	1.03024
C	-1.47618	6.25560	0.60705
H	-0.77298	6.52927	1.38336
C	0.83358	-5.26419	1.96508
H	0.60490	-6.29868	2.19064
C	0.04913	3.01771	0.00226
C	7.66199	4.39559	-1.34472
H	7.88043	5.42783	-1.58989
C	-8.58269	3.72487	1.35076
H	-9.57560	4.08660	1.58843
C	-1.19002	5.16022	-0.21929
C	8.72290	3.43935	-1.34193
H	9.72746	3.76316	-1.58527
C	-2.10449	4.83235	-1.22827
H	-1.89034	4.00762	-1.89378
C	-8.38449	2.40873	1.06711
H	-9.21318	1.71014	1.07512
C	-3.55568	6.63273	-0.54920
H	-4.47028	7.19869	-0.67592
C	-5.32687	-1.26472	-0.15685
C	0.05597	4.39307	-0.01236
C	1.56502	6.26641	-0.64918
H	0.84173	6.54623	-1.40451
C	-3.77203	-3.06648	-0.80862
H	-4.59189	-3.77199	-0.76227
C	-0.13180	-3.03735	-1.64015
H	0.68147	-2.32461	-1.69576
C	8.47995	2.13537	-1.03773
H	9.28408	1.40858	-1.03527
C	-2.65158	6.97684	0.45126
H	-2.86241	7.80955	1.11109
C	-3.27395	5.56195	-1.39135
H	-3.96815	5.29097	-2.17697
C	2.74264	6.98853	-0.51815
H	2.93387	7.82771	-1.17566

C	-2.51087	-3.51328	-1.16796
C	-0.99033	-5.29498	-1.80295
H	-0.79617	-6.34030	-2.01027
C	3.67426	6.63706	0.45409
H	4.59095	7.20374	0.56121
C	3.41612	5.55909	1.29475
H	4.13037	5.28379	2.06075
C	-6.40097	-2.18331	-0.11700
C	-2.24129	-4.88784	-1.45554
H	-3.05604	-5.59910	-1.38518
C	0.07992	-4.35524	-1.89910
H	1.06910	-4.70306	-2.16941
C	10.13530	-3.59167	-0.47380
H	10.97165	-4.29490	-0.50824
H	9.96883	-3.21452	-1.48538
H	10.42923	-2.74880	0.15602
C	8.87620	-5.03122	1.94906
H	9.14609	-4.20566	2.61124
H	7.97579	-5.50172	2.35071
H	9.68418	-5.76744	1.97716
C	8.07261	-5.84674	-0.91273
H	7.17356	-6.33397	-0.52814
H	7.85703	-5.49605	-1.92435
H	8.86404	-6.59860	-0.97490
C	-10.28189	-3.26000	-0.55729
H	-10.51148	-2.45397	0.14355
H	-10.17592	-2.82065	-1.55160
H	-11.13562	-3.94273	-0.57697
C	-8.88591	-4.84686	1.68879
H	-9.71107	-5.56202	1.74665
H	-7.97162	-5.35804	1.99853
H	-9.08063	-4.04551	2.40505
C	-8.33317	-5.54878	-1.26246
H	-8.18179	-5.15645	-2.27047
H	-7.42620	-6.08333	-0.97039
H	-9.15298	-6.27117	-1.29886

References

1. D. Lehnherr, A. H. Murray, R. McDonald and R. R. Tykwinski, *Angew. Chem. Int. Ed.*, 2010, **49**, 6190-6194.
2. T. Lange, J.-D. van Loon, R. R. Tykwinski, M. Schreiber and F. Diederich, *Synthesis*, 1996, 537-550.
3. A. R. Suárez and M. R. Mazzieri, *J. Org. Chem.*, 1987, **52**, 1145-1147.
4. J. E. Anthony, J. S. Brooks, D. L. Eaton and S. R. Parkin, *J. Am. Chem. Soc.*, 2001, **123**, 9482-9483.
5. M. Maggini, G. Scorrano and M. Prato, *J. Am. Chem. Soc.*, 1993, **115**, 9798-9799.
6. J. J. Snellenburg, S. P. Laptenok, R. Seger, K. M. Mullen and I. H. M. van Stokkum, *J. Stat. Soft.*, 2012, **49**, 1-22.
7. T. H. Dunning Jr. and P. J. Hay, in *Methods of Electronic Structure Theory*, ed. H. F. Schaefer III, Plenum Press, New York, 1997, vol. 3, pp. 1-28.
8. T. H. Dunning Jr., *J. Chem. Phys.*, 1989, **90**, 1007-1023.
9. M. B. Smith and J. Michl, *Chem. Rev.*, 2010, **110**, 6891-6936.
10. H. Nakamura and D. G. Truhlar, *J. Chem. Phys.*, 2001, **115**, 10353-10372.
11. H. Nakamura and D. G. Truhlar, *J. Chem. Phys.*, 2002, **117**, 5576-5593.
12. K. Ruedenberg and G. J. Atchity, *J. Chem. Phys.*, 1993, **99**, 3799-3803.
13. G. J. Atchity and K. Ruedenberg, *Theor. Chem. Acc.*, 1997, **97**, 47-58.